Original Paper

Cells Tissues Organs

Cells Tissues Organs
DOI: 10.1159/000209233

Accepted after revision: October 27, 2008
Published online: March 13, 2009

Efferent Projections of the Anterior and Posterodorsal Regions of the Medial Nucleus of the Amygdala in the Mouse

Kamen G. Usunoff[a–c] Oliver Schmitt[c] Dimitar E. Itzev[b]
Stefan Jean-Pierre Haas[c] Nikolai E. Lazarov[a] Arndt Rolfs[d] Andreas Wree[c]

[a]Department of Anatomy and Histology, Faculty of Medicine, Medical University of Sofia, and
[b]Institute of Neurobiology, Bulgarian Academy of Sciences, Sofia, Bulgaria; [c]Institute of Anatomy and
[d]Department of Neurology, Faculty of Medicine, University of Rostock, Rostock, Germany

Key Words
Bed nucleus of stria terminalis · Biotinylated dextran amine · Hypothalamus · Limbic system · Medial preoptic nucleus/area · Reproductive behavior

Abstract
The efferent projections of the anterior and posterodorsal part of the medial nucleus (MePD) in the mouse were studied by means of anterograde axonal tracing using biotinylated dextran amine. The MePD axons ran mainly via the stria terminalis and to a lesser extent via the ventral amygdalofugal pathway. The projections to the forebrain were broadly distributed and varied from very strong to scant. The most significant connections were destined to the bed nucleus of the stria terminalis in which all parts of the medial division were innervated by MePD neurons. Moderate projections reached the limbic striatum (nucleus accumbens), olfactory tubercle and the lateral septal nucleus. The substantia innominata was also innervated by the MePD, and especially the projection to its ventral portion was substantial. The profuse innervation of the medial preoptic nucleus and medial preoptic area indicated significant involvement of the MePD in sexual behavior. Many hypothalamic nuclei were inner-

Abbreviations used in this paper

Am	amygdaloid nuclear complex	BSTMPL	bed nucleus of the stria terminalis, medial division of the posterolateral part	MeAD	medial nucleus, anterodorsal part
AP	anteroposterior			MeAV	medial nucleus, anteroventral part
BDA	biotinylated dextran amine			Me/MeA	medial amygdaloid nucleus
BST	bed nucleus of the stria terminalis	BSTMPM	bed nucleus of the stria terminalis, medial division of the posteromedial part	MeP	medial nucleus, posterior part
BSTIA	bed nucleus of the stria terminalis, intra-amygdaloid division			MePD	medial nucleus, posterodorsal part
				MePV	medial nucleus, posteroventral part
BSTMA	bed nucleus of the stria terminalis, medial division of the anterior part	BSTMV	bed nucleus of the stria terminalis, medial division of the ventral part	MGP	medial globus pallidus
				PB	phosphate buffer
BSTMPI	bed nucleus of the stria terminalis, medial division of the posterointermediate part	DAB	3,3′-diaminobenzidine	SI	substantia innominata
		L	lateral	V	ventral
		LOT	nucleus of the lateral olfactory tract	VMH	ventromedial hypothalamic nucleus

KARGER

Fax +41 61 306 12 34
E-Mail karger@karger.ch
www.karger.com

1422–6405/09/0000–0000$26.00/0

Accessible online at:
www.karger.com/cto

Prof. Dr. Oliver Schmitt
Institute of Anatomy, Faculty of Medicine
University of Rostock, Gertrudenstr. 9, POB 100808
DE–18055 Rostock (Germany)
Tel. +49 381 494 8408, Fax +49 381 494 8402, E-Mail schmitt@med.uni-rostock.de

vated but to a different extent. The very strong innervation of the ventral premammillary nucleus further indicated the involvement of the MePD in the neuronal circuitry for sexual behavior. Substantial projections also reached the anterior hypothalamus and tuber cinereum, while the connections to the lateral hypothalamus were widespread but showed moderate density. MePD strongly innervated the ventrolateral part of the ventromedial hypothalamic nucleus and moderately its remaining parts. The neurosecretory hypothalamic nuclei and the arcuate nucleus contained only a few MePD terminals. The thalamic innervation was very scant and reached the lateral habenular nucleus and the nuclei of the midline. The mesencephalic connections were moderate to sparse and projected to the mesolimbic dopaminergic groups in the ventral tegmental area, the pars lateralis and the dorsal tier of the substantia nigra pars compacta, the periaqueductal gray and the dorsal raphe nucleus. The present results principally resembled data known in other rodent species; however, the efferents of the MePD often differed in extent and/or topical distribution.

Introduction

The amygdaloid nuclear complex (Am) is a relatively voluminous gray substance, located in the depth of the ventromedial temporal lobe, ventral to the caudolateral striatum and to the pallidum. It is a highly heterogeneous structure and consists of several nuclei, divided on the basis of cytoarchitectonic, hodological, histochemical and immunohistochemical studies [reviewed by Price et al., 1987; de Olmos, 1990; Amaral et al., 1992; McDonald, 1992; Pitkänen, 2000; McDonald, 2003; Swanson, 2003; de Olmos, 2004; de Olmos et al., 2004]. The Am has diverse afferent and efferent connections throughout the CNS, and is involved in the modulation of neuroendocrine functions, visceral efferent motor mechanisms and in complex patterns of behavior, e.g. learning and memory, aggression and defense, pain modulation, reproduction and food intake [for comprehensive reviews, see Eleftheriou, 1973; Ben-Ari, 1981; Aggleton, 1992, 2000].

The medial amygdaloid nucleus (Me, sometimes abbreviated as MeA; however, here MeA consists of MeAD and MeAV, see below) is involved in the control of sexual behavior [Wood and Newman, 1995; Newman, 1999]. The Me is comprised of several divisions: anterodorsal (MeAD), anteroventral (MeAV), posterodorsal (MePD), with intermediate nucleus, and lateral and mediate subnucleus, and posteroventral (MePV) [de Olmos et al., 1985; Paxinos and Watson, 1998; Paxinos et al., 1999; Paxinos and Franklin, 2001; de Olmos, 2004; de Olmos et al., 2004]. These Me divisions have separate afferent and efferent connections, and some of them are quite distinct [Gomez and Newman, 1992; Canteras et al., 1995; Coolen and Wood, 1998; Heeb and Yahr, 2001; Simmons and Yahr, 2002]. Also, the functional characteristics of the Me divisions appear to be different. There is growing evidence that in male animals the MePD is involved in mating behavior and ejaculation [Baum and Everitt, 1992; Coolen et al., 1998; Parfitt and Newman, 1998; Veening and Coolen, 1998; Newman, 1999; Heeb and Yahr, 2001; Simmons and Yahr, 2003], although investigation using positron emission tomography in humans provided nearly negative results concerning the Am [Holstege et al., 2003].

Despite the tremendous importance of the mouse brain especially in knock-out or knock-in animals, systematic evaluations of Am connectivity in the mostly investigated C57BL/6 mouse are rare [Barber and Field, 1975; Barber, 1982; Shipley and Adamek, 1984; Shipley and Geinisman, 1984; Smith and Millhouse, 1985; Oades and Halliday, 1987; Salazar and Brennan, 2001; Aizawa et al., 2004]. This is in so far interesting and remarkable as changes in the behavior of genetically altered mice were discussed in comparison to connections described mostly in the rat. Therefore, studies providing identical projection patterns of mice and rats are demanded. Here, we report data on the efferent connections of the mouse MeA and MePD that often differ in extent and/or topical distribution from the results known from the rat, hamster and gerbil.

Materials and Methods

Twelve young-adult male mice (C57BL/6J, Charles River, Sulzfeld, Germany), weighing 18–20 g, were used. All housing facilities and procedures were carried out in accordance with the Bulgarian and German regulations on animal welfare and were consonant with the guidelines established by the National Institutes of Health (NIH Publ. No. 80-23). The mice were anesthetized with ketamine (75 mg·kg^{-1}) and Rompun (5.8 mg·kg^{-1}). After mounting, the animal was placed in a rat stereotactic frame (David Kopf, Tujunga, Calif., USA) equipped with a mouse adaptor (Stoelting, Wood Dale, Ill., USA), with the skull in flat position, and 0.25 μl biotinylated dextran amine (BDA, molecular weight 10 kDa; Molecular Probes Europe, Leiden, The Netherlands), 10% solution dissolved in phosphate buffer (PB; 0.1 M, pH 7.2), were injected unilaterally into the Me (n = 10) using a vertical approach. In order to control the specificity of the Me projections, the same amount of tracer was injected in the medial globus pallidus (MGP), often designated 'entopeduncular nucleus' in subprimate species (n = 2). Stereotactic coordinates were obtained

from the atlas of Paxinos and Franklin [2001]. Based on the bregma, the coordinates for the Me were anteroposterior (AP) –1.5, lateral (L) 1.8 and ventral (V) –5.2 and for the MGP they were AP –1.3, L 1.8 and V –4.5. The BDA solution was freshly prepared each day of injection. The tracer was injected (0.05 μl/min) using a Hamilton (5 μl) syringe supplied with a glass micropipette, the outer diameter of the tip being approximately 80 μm. At the end of the injection, the pipette was held in place for 15 min to insure absorption of the injected tracer into the tissue. After a survival time of 14 days, the animals were deeply reanesthetized with ketamine and Rompun and perfused transcardially with 10 ml of 0.9% saline, followed by 50 ml of 4% paraformaldehyde in PB. The brains were removed, postfixed in the same fixative overnight and transferred to 1% paraformaldehyde in 20% sucrose in PB until they sank. Free-floating, serial sections cut at a thickness of 40 μm on a Jung freezing microtome were collected in PB containing 0.1% Triton X-100 and placed on a rocking table overnight.

The sections were preincubated with PB containing 0.1% bovine serum albumin (fraction V; Sigma, St. Louis, Mo., USA) and 0.3% Triton X-100 for 30 min, and rinsed in three baths of PB to which 0.3% Triton X-100 was added for 30 min. A commercially available avidin-biotin-horseradish peroxidase complex was used to visualize BDA (Vectastain® ABC kit; Vector Laboratories, Burlingame, Calif., USA). To 20 ml of PB, four drops of solution 'A' and four drops of solution 'B' were added 30 min before use. The sections were incubated in the ABC kit for 60 min followed by rinsing in PB for a total of 30 min. The reaction product was developed with 0.06% 3,3′-diaminobenzidine (DAB; Sigma) and 0.02% H_2O_2 in Tris buffer (0.05 M, pH 7.6). The sections were preincubated in DAB solution for 10 min and then transferred to a DAB solution to which H_2O_2 was added for further 10 min. They were rinsed thoroughly in distilled water, mounted on chrome-alum-subbed slides and dried overnight. The sections were counterstained with 0.1% cresyl violet (Sigma), dehydrated through graded ethanol series, cleared in xylene and coverslipped with Entellan® (Merck, Darmstadt, Germany). The sections were examined using Nikon BX-51 and Leitz Aristoplan microscopes. Photomicrographs of selected fields were taken with a digital camera (7.3 three Shot Colour; Visitron Systems/Diagnostic Instruments, Puchheim, Germany).

Results

The following paragraphs introduce several phrases describing the morphological entities that contain BDA. A short definition of these expressions is provided below. An *Axon or nerve fiber* is a projection of a neuron that conducts electrical impulses away from the neuronal soma. *Axon terminals or terminals* are those parts of an axon that do not branch and where the axon ends. A *terminal field* consists of several terminals of an axon that are lying close together in a small volume of tissue. The densities of terminals and projections that are described in the following paragraphs are summarized in serial sections in figure 13.

Topography of Me Subdivisions

In the mouse, the Me measured approximately 1.6 mm rostrocaudally. Its caudal pole was represented by small sectors of the MePD and MePV (fig. 1a). Medial to the MePD was the optic tract; dorsally, most posterior fibers of the emerging stria terminalis were located, and laterally the caudalmost sector of the intra-amygdaloid division of the bed nucleus of the stria terminalis (BSTIA) was found. Medially, the MePV reached the brain surface. Ventral to it, in some sections, a very small sector of the dentate gyrus appeared. Ventrolateral to the MePV was the posteromedial cortical nucleus of the Am, and laterally there was the anterolateral portion of the amygdalohippocampal area. In rostral direction (fig. 1b), both divisions of the posterior part of the medial nucleus (MeP) enlarged, especially the MePD, which extended from dorsolateral to ventromedial, bordered medially by the optic tract. Dorsomedial to the MePD was the MGP and dorsolateral the central nucleus of the Am. Lateral to the MePD were the intercalated nuclei of the Am and BSTIA (dorsally), and the basomedial nucleus of the Am (ventrally). The MePV reached the brain surface. Lateral to it, there were the ventral portion of the basomedial nucleus and the anterior cortical nucleus. Both MePD and MePV displayed subpially a cell-poor zone (quasi a 'molecular layer'), but deeper the medium-sized neurons were densely arranged. The MeA had slightly smaller rostrocaudal dimensions. Somewhat arbitrarily, it might also be subdivided in MeAD and MeAV. The latter group was very small in the mouse, and it was not present through the entire rostrocaudal extent of the MeA. Slightly more densely arranged neurons were found compared with the MeAD. Caudally, the posterior portion of the MeA (fig. 1c) merged imperceptibly with the MePD and MePV. Medial to it was the optic tract and ventromedially, the MeA reached the brain surface. Dorsal to the MeA was a thin layer of substantia innominata (SI), wedged between the internal capsule and the optic tract. Lateral to the MeA were the basomedial nucleus (dorsally) and the anterior cortical nucleus (ventrally). The MeA did not display a distinct 'molecular layer'. The rostral pole of the MeA (fig. 1d) was composed of more loosely arranged and larger neurons. Medial to the MeA was the supraoptic nucleus, dorsally the SI and laterally the nucleus of the lateral olfactory tract (LOT). The border to the LOT was very distinct, but the transition towards SI and the ventral division of the anterior Am (rostrally) was not sharply delineated.

Injection Sites in the Me

Although all injection foci involved the Me, and the amount of tracer was theoretically constant, the injection

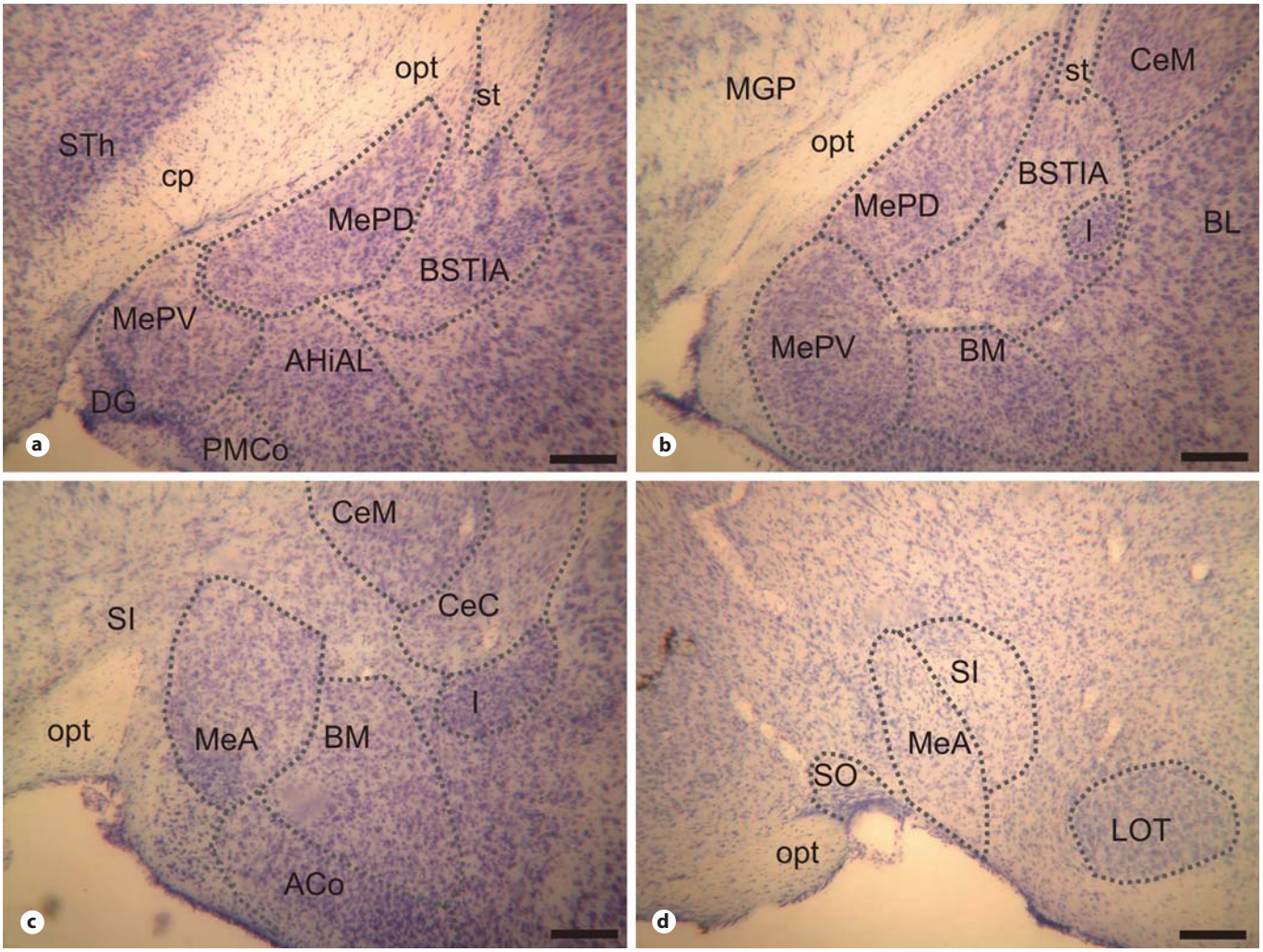

Fig. 1. Four serial sections through the Am stained with cresyl violet. Medial is to the left. **a** Section near the caudal pole of the Me. AHiAL = Amygdalohippocampal area, anterolateral part; cp = cerebral peduncle; DG = dentate gyrus; opt = optic tract; PMCo = posteromedial cortical nucleus; st = stria terminalis; STh = subthalamic nucleus. **b** Section through the maximum extent of the MePD and MePV. BL = Basolateral amygdaloid nucleus; BM = basomedial amygdaloid nucleus; CeM = central amygdaloid nucleus, medial part; I = intercalated nuclei. **c** Section through the maximum extent of the MeA. ACo = Anterior cortical nucleus; CeC = central amygdaloid nucleus, capsular part. **d** Section through the rostral pole of the Me. SO = Supraoptic nucleus. Scale bar: 200 μm.

Fig. 2. Injection foci and intra-amygdaloid projections of the MePD. In this, as well as in the remaining figures, medial is to the right. **a** Injection focus in the MePD. **b** Injection focus in the MeA-MePD border. **c** Enlargement of **a**. From the lateral aspect of the injection focus, an associated intra-amygdaloid bundle ran in dorsolateral direction towards the nuclei shown in **f** and **g**. **d–f** Dense terminal fields in the MePV (**d**), MeA (**e**; several retrogradely labeled neurons were also seen), BSTIA (**f**; outlined) and in the intercalated nuclei (**f**). **g** Dense terminals in the central nucleus, capsular part (outlined). **h–j** Injection focus of case 1 in the MeA (**h**), case 2 in the MeA (**i**) and of case 3 in the lateral portion of the central rostrocaudal MePD close to the stria terminalis (**j**). Scale bar: 200 (**a**, **b**) and 50 μm (**c–g**).

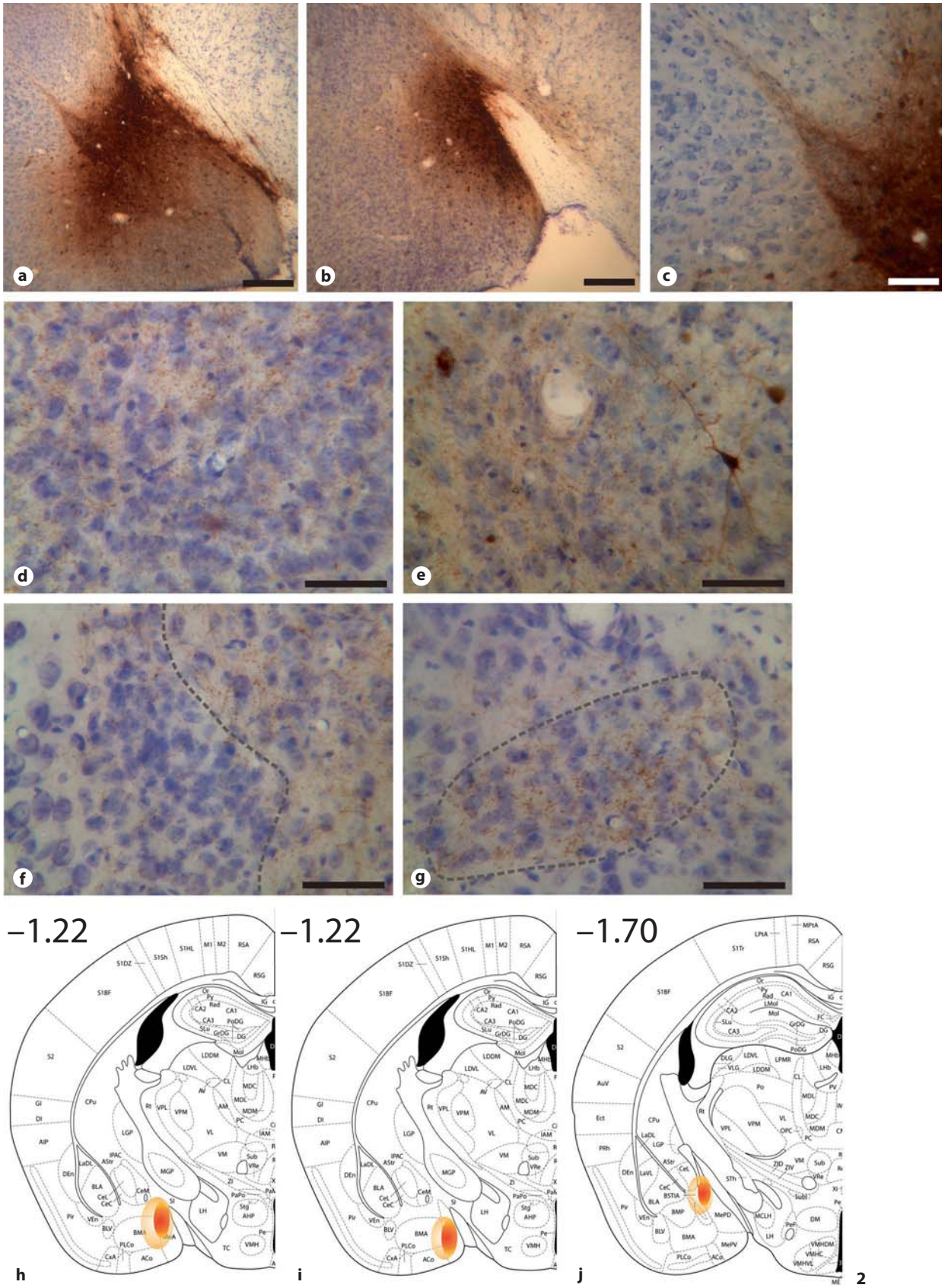
a
b
c
d
e
f
g
–1.22
–1.22
–1.70
h
i
j
2

foci differed in volume: from small to more voluminous that encroached over adjacent Am nuclei. We decided to perform a rigorous selection of only 3 cases of a total of 10 animals exhibiting selective injection foci in the Me (fig. 2). All injection foci were displayed schematically in figure 2h–j. In cases 1 and 2, these foci were placed in the posterior part of the MeA close to the boarder of the MePD (MeA-MePD borderline; fig. 2b). These foci clearly displayed extensions into the rostral portions of the MePD of cases 1 and 2. Because of these extensions of the BDA into the MePD, these cases were evaluated. In case 3, one focus was placed in the central portion of the MePD (cf. fig. 1a, b), involving mainly its lateral portion, close to the emerging stria terminalis. No case with a selective injection in the ventral sectors (MeAV) of the Me was obtained. In summary, 3 animals (cases 1–3) were evaluated: the borderline MeA-MePD injections (cases 1 and 2) and the MePD injection (case 3).

Efferent Projections of the MePD

Intra-Amygdaloid Connections

From the injection foci, axons destined to other Am nuclei emerged. Dense terminal fields were observed in the other Me sectors, MePV (fig. 2d) and MeA (fig. 2e), in which retrogradely labeled neurons were also present. From the lateral aspect of the injection focus, a delicate but distinct bundle arose (fig. 2c) that reached the small, compactly arranged neurons of the intercalated Am nuclei and the surrounding BSTIA (fig. 2f). A variable number of terminals was present in the central amygdaloid nucleus (mainly in the capsular and medial divisions, fig. 2g) and in the basomedial nucleus. Occasionally, axons were traced to the anterior Am and to the cortical nuclei but not to the LOT. Also, in cases with voluminous injections in the Me, not a single axon was traced among the largest Am neurons, building the basolateral nucleus.

Projections to the Forebrain

The extra-amygdaloid efferent connections of the MePD followed two routes: the stria terminalis (fig. 3a) and a bundle that curved medially over the optic tract (a component of the 'ventral amygdalofugal pathway' or 'ansa peduncularis' in higher species). The distinctly labeled axons of the stria terminalis were located in its medial part curving around the optic tract and the cerebral peduncle ventrally, and the reticular thalamic nucleus dorsally. The supracapsular portion of the stria terminalis bent in a rostral direction, occupying the groove between the most dorsal neostriatal islands and the dorsolateral thalamus (fig. 3b). The second component was smaller but its ventral part was also very distinct (fig. 3c, d). These axons, after a short intra-amygdaloid course in rostral direction, left the medial aspect of the Am and ran medially immediately dorsal to the optic tract, reaching the midline and then the continuing line for a short distance in the contralateral hemisphere. The number of such axons was most prominent at the level of the suprachiasmatic nucleus (fig. 3c), but few labeled axons might also be followed at retrochiasmatic level, ventral to the ventromedial hypothalamic nucleus (VMH), and a fair number of labeled axons covered dorsally also the most rostral portion of the optic chiasm (fig. 3d).

At prethalamic level, the stria terminalis abruptly descended (fig. 3e, f). The labeled axons ran from the supracapsular stria terminalis through the bed nucleus of the stria terminalis (BST), medial division, posteromedial part (BSTMPM), adjacent to the posterointermediate part (BSTMPI; fig. 3f). From the BST subdivisions, the largest number of labeled axons and terminals was observed in the BSTMPM (fig. 4a) and BSTMPI (fig. 4b). The anterior portions of the BST, medial division, posterolateral part (BSTMPL), contained a moderate number of terminals (fig. 4b), but the posterior sectors of the

Fig. 3. Major efferent pathways of the MePD (case 3). **a** The stria terminalis ascended in the coronal plane. BDA-labeled axons were located in its medial part. opt = Optic tract; Rt = reticular thalamic nucleus; VPL = ventral posterolateral thalamic nucleus; VPM = ventral posteromedial thalamic nucleus. **b** In the supracapsular portion of the stria terminalis, BDA-labeled axons were located ventromedially. fi = Fimbria of the hippocampus; ic = internal capsule; Str = striatum. **c** A compact bundle of labeled axons ran towards the midline above the posterior portion of the optic chiasm. LA = Lateroanterior hypothalamic nucleus; MPA = medial preoptic area; Sch = suprachiasmatic nucleus; 3v = third ventricle. **d** A delicate, more loosely arranged bundle of labeled axons crossed the midline at the level of the most rostral part of the optic chiasm (ox). **e** The stria terminalis (upper left part of the figure) immediately before its prethalamic descent still contained a compact bundle of labeled axons. The section corresponds to figure 35 in Paxinos and Franklin [2001]. f = Fornix; LGP = lateral globus pallidus; LH = lateral hypothalamus; sm = stria medullaris. Enlargements from this figure are given in figure 4c, d and figure 6a. **f** Descent of the stria terminalis, dispersing its labeled axons within the BST subnuclei. This section corresponds to figure 33 in Paxinos and Franklin [2001]. The main stream of labeled axons ran in the lateral division of the posterior part of the BST, the medial division of the posteromedial part of the BST, the BSTMPL and the BSTMPI. A smaller bundle curved medially under the ependyma and descended along the medial border of the BSTMPM. Enlargements from this figure are given in figure 4a, b. Scale bar: 200 (**a**, **b**, **e**, **f**) and 100 μm (**c**, **d**).

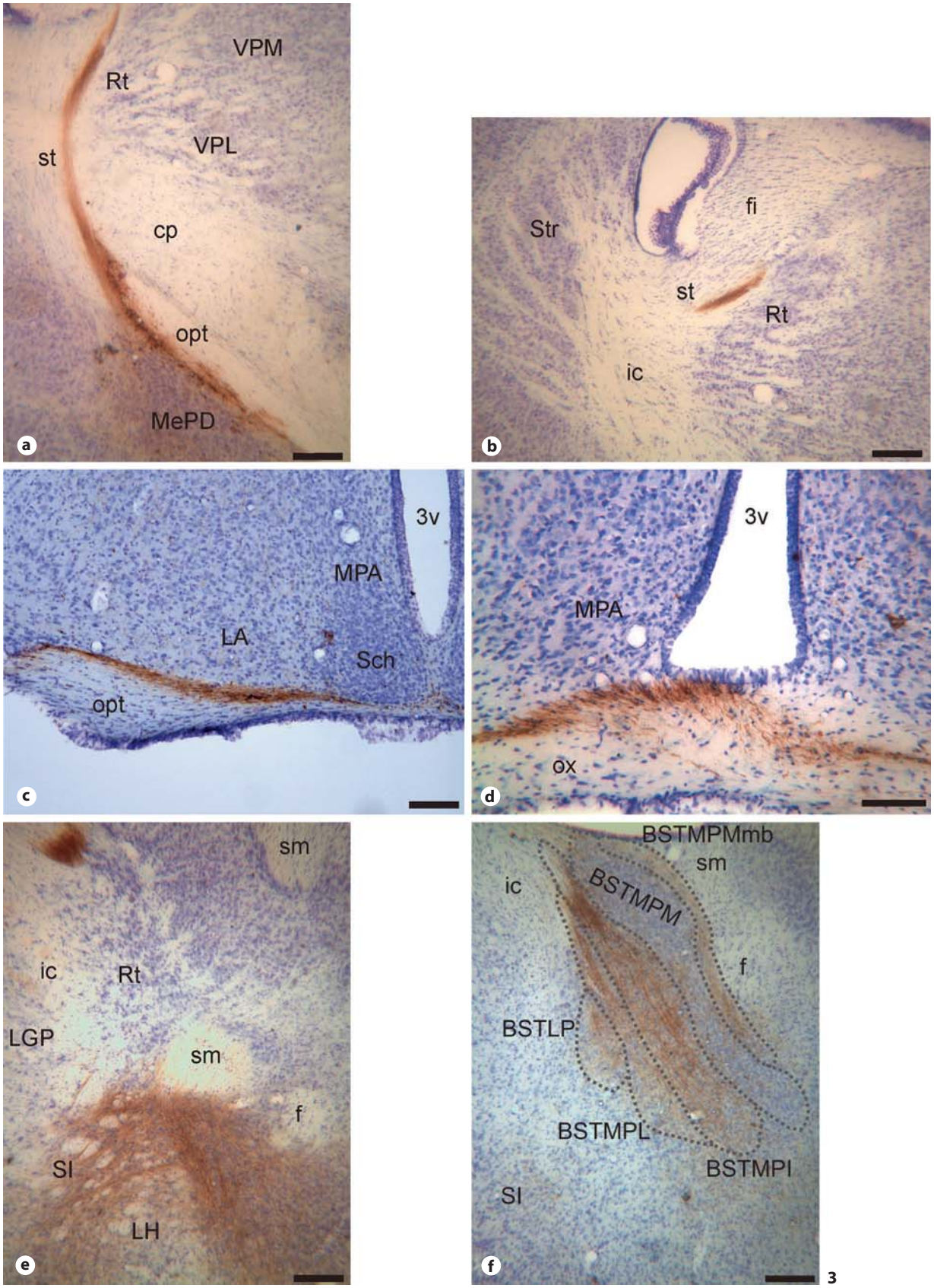
VPM
Rt
st
VPL
cp
opt
MePD
a
Str
fi
st
Rt
ic
b
3v
MPA
LA
Sch
opt
c
3v
MPA
ox
d
sm
ic
Rt
LGP
sm
f
SI
LH
e
BSTMPMmb
sm
ic
BSTMPM
f
BSTLP
BSTMPL
BSTMPI
SI
f

3

BSTMPL surrounding the ventral aspect of the fornix contained a large number of labeled fibers (fig. 4c). Immediately lateral to this field, in the region nominated 'nucleus of stria medullaris' by Paxinos and Franklin [2001], an extremely dense field of termination was observed (fig. 4d). In conjunction with the latter field, a large number of labeled axons were followed within the stria medullaris (fig. 4d). At the level of the crossing of the posterior aspect of the anterior commissure by the fornix columns, the labeled stria terminalis axons dispersed in dense terminal fields within the most caudal portions of the BST, medial division, anterior part (BSTMA), and BST, medial division, ventral part (BSTMV; fig. 4e, f). The labeled axons did not enter the sharply delineated bed nucleus of the anterior commissure. Slightly more rostrally, the terminals were distributed in the BSTMA and BSTMV, and both fields were interconnected by labeled axons that vertically crossed the axons of the anterior commissure (fig. 4g). The labeled strial axons also projected to the most rostral regions of the BST, surrounding the anterior commissure axons that turned in rostral direction and pierced the nucleus accumbens. The labeled axons surrounded the medial aspect of the anterior commissure (fig. 4h).

A substantial number of labeled axons were encountered in the nucleus accumbens core, especially in the shell (fig. 5a, b). Medially, the labeled axons reached the major island of Calleja (the 'insula magna'). Some axons coursed around the medial aspect of the major island and ramified sparsely within the cell-poor region of the intermediate part of the lateral septal nucleus (fig. 5c, e). In the insula magna, only few terminal ramifications were found, mainly at its dorsal and ventral corners (fig. 5c, e). Ventrally, the nucleus accumbens shell was followed by labeled axons. They reached the Calleja islands ('insulae minores') and some terminals were observed in their neuropil (fig. 5d, f). A larger number of labeled terminals were seen in the deeper portion of the olfactory tubercle (fig. 5d, f), and some scattered axons were noted towards the superficial portions (fig. 5d).

In the ventral part of the lateral septal nucleus, a moderate number of terminals was seen (fig. 5g). The terminal arborizations built discrete patches, often arising from a single axon. A large number of axons was seen in the septofimbrial nucleus (fig. 5h). They ran parallel to each other towards the triangular septal nucleus but did not end with terminal fields.

At caudal BST levels, the robust stream of labeled axons split ventral to the BSTMPL in two components (fig. 3e). A smaller, loosely arranged bundle bent laterally and coursed ventral to the internal capsule towards the SI, intermingled with unlabeled axonal fascicles (fig. 6a). Some axons also extended to the SI through the ventral amygdalofugal pathway. All SI subdivisions contained labeled axons and terminals. The small but compact bundles dispersed within the ventral portion of the SI (fig. 6b). Terminals were rare, but the axons of the passage displayed numerous varicosities along their course. Dorsally, most of the labeled axons ramified very sparsely. Some of them passed close to large, chromophilic neurons of the basal magnocellular nucleus of Meynert, but did not arborize intensively in their vicinity (fig. 6c). A mighty bundle continued ventrally-ventromedially towards the anterior hypothalamus, medial preoptic nucleus and medial preoptic area (fig. 3e). From the most proximal part of this bundle, some labeled axons deviated medially. They surrounded the ventral aspect of the fornix and terminated within the anterodorsal preoptic nucleus (fig. 6d).

All medial preoptic structures contained a substantial number of labeled axons and terminals: the medial and lateral subdivisions of the medial preoptic nucleus, as well as the medial preoptic area (fig. 6e, f). Medial to the medial preoptic nucleus (dorsally) and medial preoptic area (ventrally), the terminal field extended subependy-

Fig. 4. Distribution of labeled axons and terminals within the BST. **a**, **b** Enlargements from figure 3f. **a** The two descending bundles emitted numerous axon terminals within the BSTMPM. **b** Numerous axons and terminals in the BSTMPI. The rostral portion of the BST, the BSTMPL, contained a moderate number of terminals. **c**, **d** Enlargements from figure 3e. **c** A substantial number of labeled axons and terminals in the posterior part of the BSTMPL, surrounding the ventrolateral aspect of the fornix (cf. **b**). **d** Numerous labeled axons (both of passage and terminal ones) in the nucleus of the stria medullaris (lower part of the figure). Dorsally, a substantial number of loosely arranged labeled axons presented in the stria medullaris (sm). **e** Fornix columns crossed the posterior aspect of the anterior commissure (ac). BAC = Bed nucleus of the anterior commissure; BSTLI = BST, lateral division, intermediate part; D3V = dorsal part of the third ventricle; LSV = lateral septal nucleus, ventral part; LV = lateral ventricle. **f** Enlargement from **e**. Dense terminal fields in the posterior portions of the BSTMA (upper part of the figure) and BSTMV (lower part of the figure). No terminals were found among the densely arranged, hyperchromic neurons of the bed nucleus of the anterior commissure. **g** Terminal fields in more anterior portions of the BSTMA and BSTMV. To the left: labeled axons crossed vertically the compact fiber bundle of the anterior commissure. **h** Most rostral axons and terminal fields in the BSTMA and BSTMV merged medial to the anterior commissure. The labeled axons swept along its medial aspect. Scale bar: 50 (**a–d**, **g**, **h**), 200 (**e**) and 100 μm (**f**).

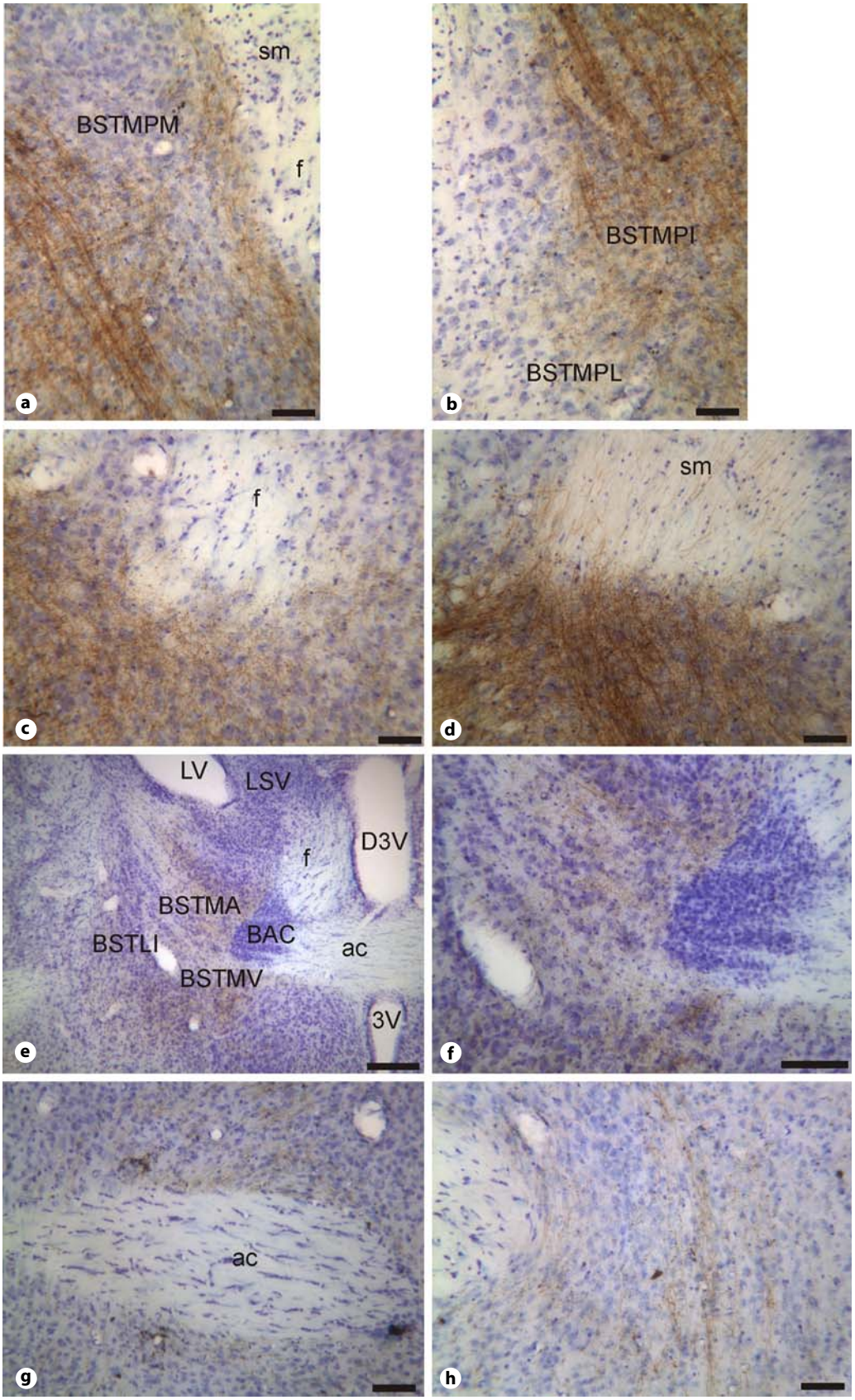
sm
BSTMPM
f
a
BSTMPI
BSTMPL
b
f
c
sm
d
LV
LSV
D3V
f
BSTMA
BAC
BSTLI
ac
BSTMV
3V
e
f
ac
g
h

4

mally in the periventricular hypothalamic zone. Lateral to the MPA, the terminal field imperceptibly continued within the subdivisions of the anterior hypothalamus.

The pathways to the VMH deserve special attention because the data available indicated that anterior and posterior Me portions emitted drastically different projections towards this nucleus (see Discussion). In the case with the selective MePD injection, the lateral and ventral borders of the VMH were surrounded by dense terminal fields that also occupied the VMH ventrolateral subnucleus. A substantial number of terminals was also present in the central subnucleus, and even the dorsomedial subnucleus contained a moderate number of terminals (fig. 7a). In contrast, in the cases with main tracer infiltration in the MeA, the entire VMH was filled with axonal terminals with such an enormous density that the borders of the nucleus were sharply outlined (fig. 7b). In these cases, some terminals were also noted in the contralateral VMH, too.

The labeled terminal fields in the lateral hypothalamus and in tuber cinereum arose primarily from axons running within the ventral amygdalofugal pathway. In the lateral hypothalamus, the labeling pattern tended to be patchy, with alternating fields of scant and moderate labeling (fig. 7c). As described above, the initial part of the 'pars tecta' of the fornix columns was surrounded by a dense terminal field in the BSTMPL. Further descending fornix fibers were surrounded by labeled terminals, from the rostral part of the lateral hypothalamus to the fornix fibers in the caudal part of the lateral hypothalamus (fig. 7d), where they were surrounded by the perifornical nucleus [Paxinos and Franklin, 2001]. In the tuber cinereum, the number of labeled axons and terminals was substantial and diminished only in the most superficial, subpial zone (fig. 7e).

Innervation of the neurosecretory hypothalamic nuclei appeared to be very scant. As a rule, the dorsal border of the supraoptic nucleus was surrounded by a dense plexus of labeled axons, but extremely rarely such axons entered the neuropil of the supraoptic nucleus (fig. 7f). The paraventricular nucleus was surrounded by numerous labeled axons in the central and posterior portions of the anterior hypothalamic area (fig. 8a, b), but only few axons arborized among the paraventricular nucleus neurons (fig. 8c).

In the ventrocaudal hypothalamus, a very dense field of labeled terminals was observed in the ventral premammillary nucleus (fig. 8d, e). Since the number of labeled parent axons approaching this area was low, apparently these axons possibly arborized profusely within the ventral premammillary nucleus. Few labeled axon terminals presenting with extremely thin intervaricose portions were observed within the lateral posterior and medial posterior divisions of the arcuate nucleus (fig. 8d, f).

The selective injections in the MeA-MePD border and MePD resulted in very scant labeling in several thalamic and epithalamic nuclei. Axons from the stria medullaris were followed to the lateral habenular nucleus (fig. 9a). Discrete terminal patches were located in its lateral part, and individual terminals were also seen medially, adjacent to the medial habenular nucleus (fig. 9b). Several nuclei of the midline exhibited a very limited number of labeled terminals, the axons apparently ascending from the dorsal hypothalamus. Terminals were comparatively more constantly found in the nucleus reuniens (fig. 9c), some even in the contralateral nucleus reuniens (fig. 9d). Dorsally, individual axonal clusters were observed in the rhomboid thalamic nucleus (fig. 9e), and scattered terminals appeared in the interanteromedial thalamic nucleus (fig. 9f). Notably, the cases with injections involving mainly the MeA-MePD border revealed not very different findings. The terminal field in the lateral habenular nucleus was more distinct (fig. 9g; this was the main reason to perform also control injections in the MGP), and some labeled axons appeared also in the paraventricular and parataenial thalamic nuclei, and in the zona incerta (fig. 9h).

Fig. 5. Distribution of labeled axons and terminals in the nucleus accumbens, islands of Calleja, olfactory tubercle and septal nuclei. **a** To the left: nucleus accumbens (Acb), surrounding the anterior commissure; in the center: the vertically oriented major island of Calleja (ICjM); to the right: intermediate part of the lateral septal nucleus (LSI). ac = Anterior commissure. **b**, **c**, **e** Enlargements from **a**. **b** A dense terminal field in the ventromedial part of the nucleus accumbens shell (AcbSh; lower right) and a moderate number of terminals in the nucleus accumbens core (AcbC; upper left). **c** Labeled axons ran medial and lateral to the ventral part of the 'insula magna' of Calleja but only few axons entered it. **d** Medial part of the olfactory tubercle. Ventral to an island of Calleja (ICj), there was a horizontally oriented terminal field in the deep portion of the olfactory tubercle. Scattered axons and terminals were also seen in the superficial portions of the olfactory tubercle. **e** Labeled axons and terminals in close proximity to the dorsal 'wedge' of the major island. **f** Enlargement from **d**. Thin labeled axons in the olfactory tubercle. Some terminals were also seen among the aggregated neurons of the island of Calleja. **g** Scattered axon terminals in the ventral part of the lateral septal nucleus. **h** Labeled axons of the passage into the septofimbriate nucleus (SFi) running towards the triangular septal nucleus (TS). Scale bar: 100 (**a**) and 50 μm (**b**–**h**).

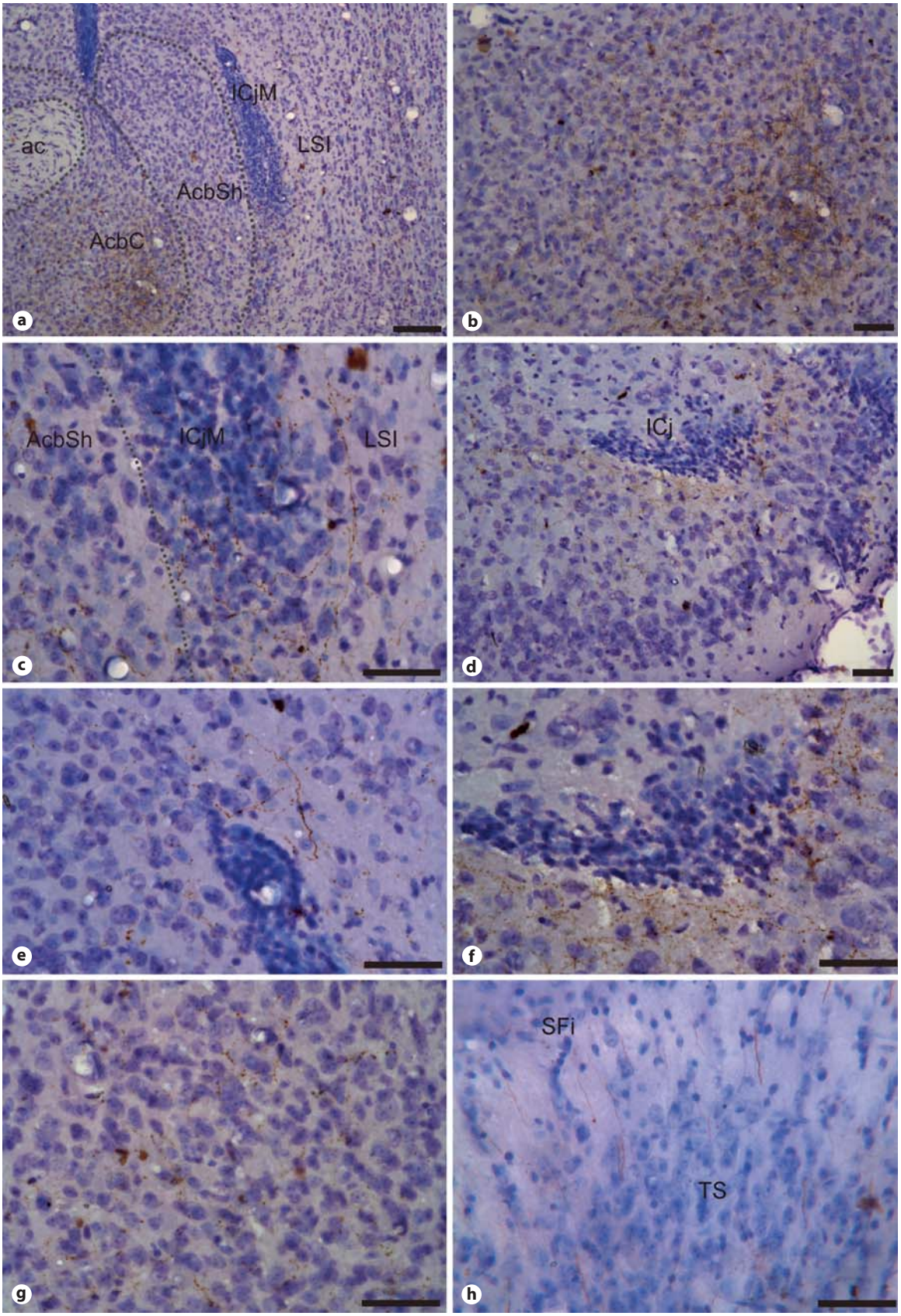

5

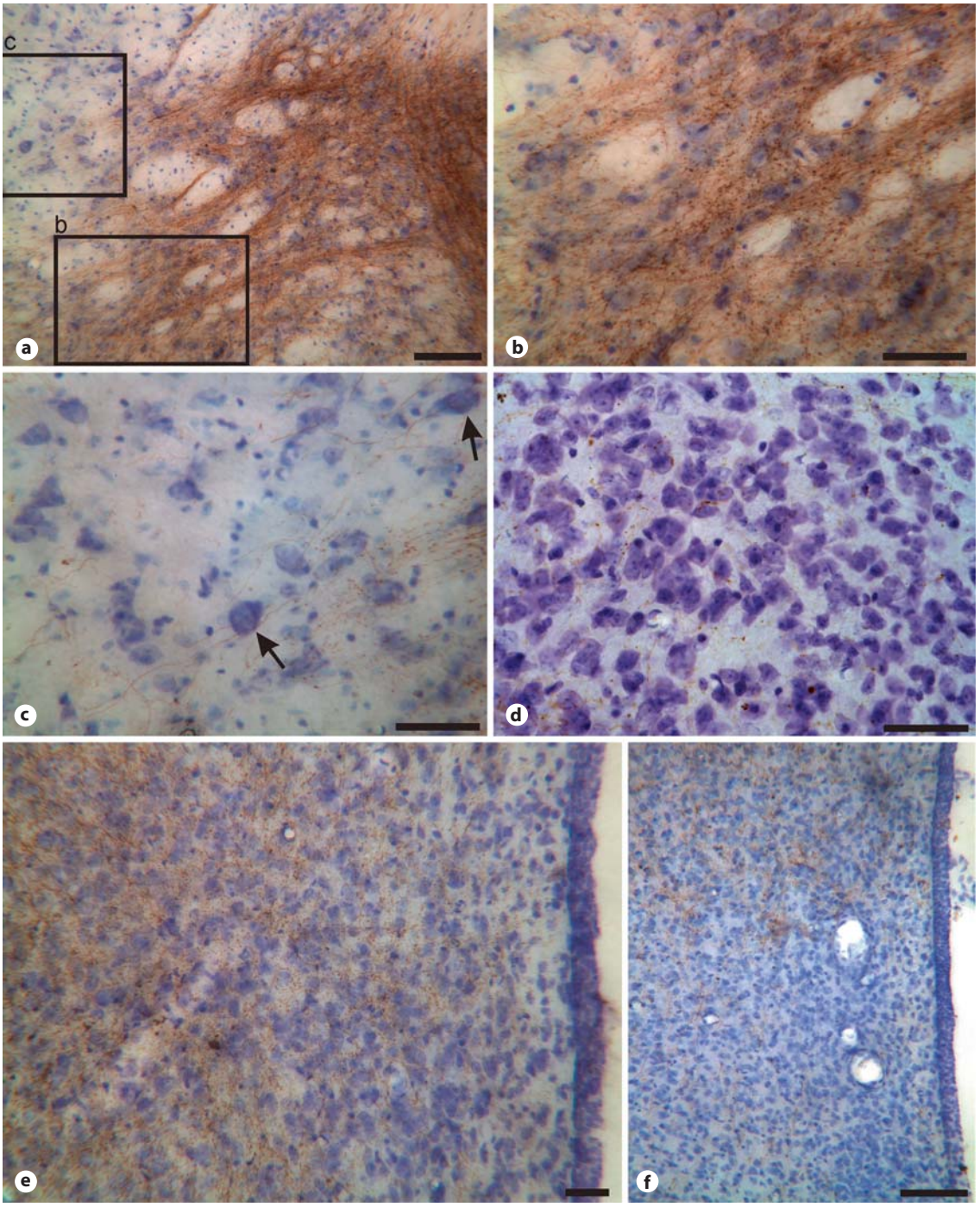

Fig. 6. Projections towards the SI and medial preoptic regions. **a** Enlargement from figure 3e. Bundles of labeled axons coursing laterally to the SI. **b**, **c** Insets from **a**. **b** The compact bundles dispersed within the ventral portion of the SI. Terminals were rare, but passage axons also displayed numerous varicosities. **c** Dorsally, SI cells were loosely arranged, interstitial to the most ventral axons of the internal capsule. The two larger, chromatophilic neurons (arrows) might represent dispersed Meynert's neurons. Most of the labeled axons were fibers of passage, although to the lower right a sparse terminal field was also present. **d** Scattered terminals in the anterodorsal preoptic nucleus. **e** Very dense, homogenous terminal field in the lateral subnucleus of the medial preoptic nucleus (to the left) and a substantial number of terminals in the medial subnucleus. Few terminals were also present in the oligocellular subependymal region. **f** This photograph is from the section shown at low magnification in figure 3c. Substantial density of labeled terminals in the medial preoptic area. Towards the suprachiasmatic nucleus (lower part of the figure), the density of the field slightly diminished. Scale bar: 100 (**a**, **f**) and 50 μm (**b**–**e**).

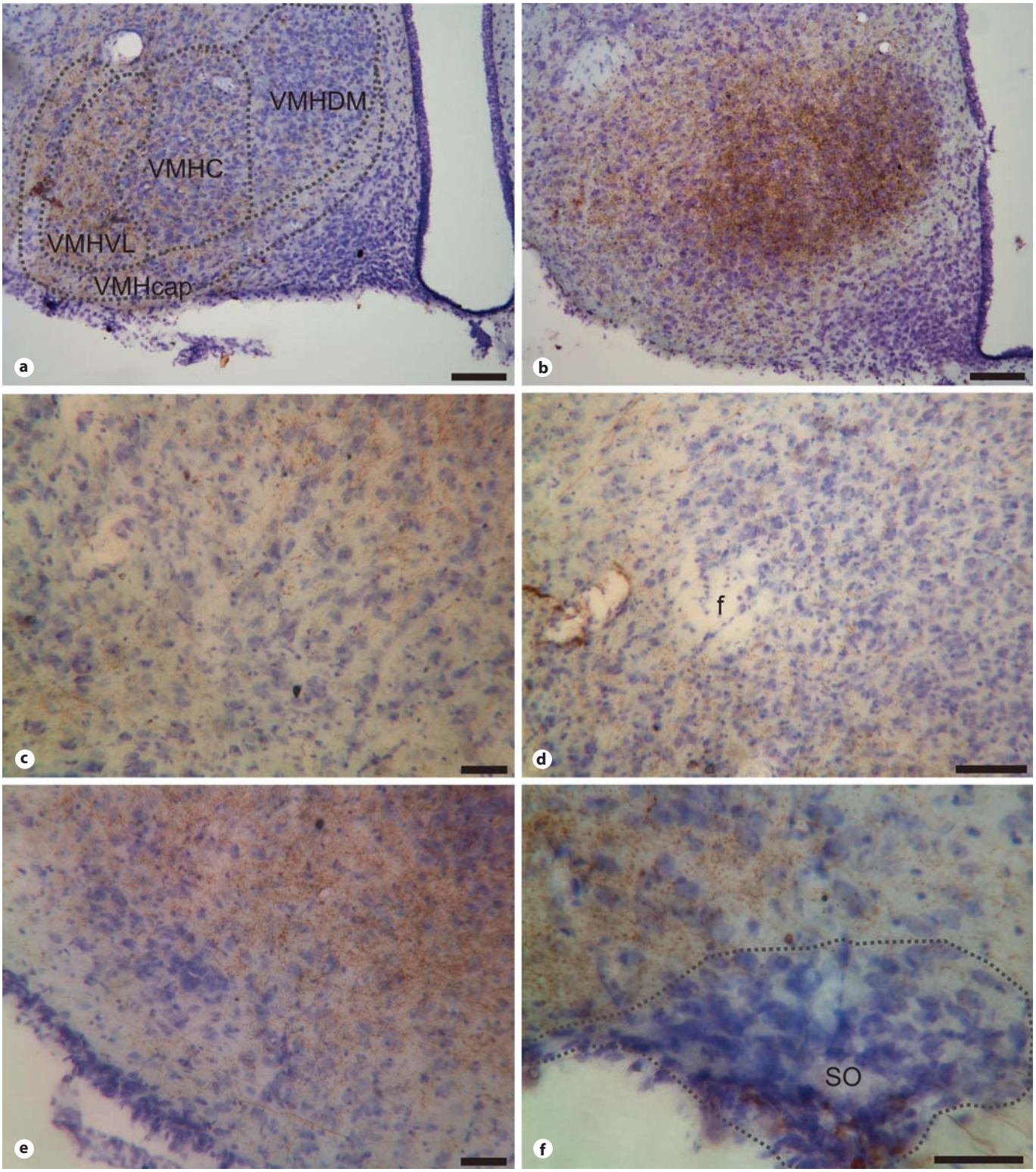

7

(For legend see next page.)

Projections to the Brainstem

Moderate projections from the MePD were traced to the rostral brainstem. The labeled axons ran through the caudalmost lateral hypothalamus in the groove between the medial border of the cerebral peduncle and the lateral mammillary nucleus (fig. 10a), and entered the ventral zone of the rostralmost ventral tegmental area (fig. 10b). The labeled axons spread over the entire dopaminergic nuclear complex, but none of the innervated structures exhibited a substantial number of terminals. In the substantia nigra, axon terminals were seen in the pars lateralis (fig. 10c) and in the dorsal tier of the pars compacta (fig. 10d). In the ventral tegmental area, scattered terminals were encountered in the paranigral, interfascicular and rostral linear nuclei (fig. 10e–g). A loose bundle of labeled axons ran dorsally in the tegmentum and entered the lateral portion of the periaqueductal gray (fig. 11a, b). The labeled terminals formed discrete patches that almost reached the ependyma of the aqueduct (fig. 10c). In the dorsal raphe nucleus, only very few terminals were observed (fig. 10d). The results of the present investigation are summarized in table 1.

Projections of the MGP

In both cases, BDA was successfully injected in the MGP. In one of the cases, the injection focus was very discrete (fig. 12a). It involved only a relatively small portion of the MGP, and the tracer infiltrated the characteristic neuropil network of the MGP leaving the corticofugal axons unlabeled. Although only a small number of pallidal neurons were infiltrated, the efferent connections of the MGP were successfully traced. A dense terminal field was observed in the ipsilateral lateral habenular nucleus (fig. 12b), ventromedial thalamic nucleus (fig. 12c) and parafascicular nucleus (fig. 12d). A small number of axons was traced to the ipsilateral pedunculopontine tegmental nucleus, mainly to its pars dissipata, associated with the axons of the decussating superior cerebellar peduncle (fig. 12e). An unexpected finding was the presence of a fairly dense terminal field in the ipsilateral red nucleus (fig. 12f).

Discussion

Methodological Considerations

Two types of BDA are used as neuronal tracers: 'light' [3,000 kDa (BDA3k)] and 'heavy' [10,000 kDa (BDA10k)]. BDA3k is an excellent retrograde tracer but not the tracer of choice for anterograde tracing. On the other hand, BDA10k is highly recommended as an anterograde tracer, and it does yield some retrograde labeling [Reiner et al., 2000, and references therein]. Other benefits of BDA10k are that it might be combined with established retrograde tracers, such as cholera toxin B and Fluoro-Gold [Coolen and Wood, 1998; Coolen et al., 1999; Lanciego et al., 2000], and that BDA tracing at ultrastructural level is also possible, in particular in combination with transmitter immunocytochemistry [Pickel et al., 1996; Reiner et al., 2000; Miyashita et al., 2007]. We confirm that BDA10k might be the tracer of choice for anterograde tracing experiments. The injection foci are selective and sharply localized, thereby making it possible to confine the injection to the region of interest and to study the topographic

Fig. 7. Projections to the hypothalamus. **a** Terminal field in the VMH following a selective BDA injection in the MePD. Dense terminal fields were noted lateral and ventral to the VMH ('capsule' of VMH: VMHcap) as well as in the ventrolateral subnucleus of the VMH (VMHVL). Slightly smaller condensation of terminals in the central subnucleus (VMHC). Only a moderate number of labeled terminals was observed in the dorsomedial subnucleus (VMHDM). **b** Terminal field in the VMH following a selective injection in the MeA-MePD border. A very dense terminal field occupied the entire territory of the VMH. **c** Moderate, patchy labeling in the lateral hypothalamus. **d** Perifornical localization of labeled terminals in the posterior part of the lateral hypothalamus. f = Fornix. **e** Numerous terminals in tuber cinereum. The density of the field diminished towards the ventral brain surface. **f** Numerous terminals immediately dorsal to the supraoptic nucleus (SO) containing only occasionally terminals in its periphery. Scale bar: 100 (**a**, **b**) and 50 μm (**c–f**).

Fig. 8. Projections to the hypothalamus. **a** A dense terminal field in the central portion of the anterior hypothalamus abutting the lateral border of the paraventricular hypothalamic nucleus, ventral part, containing only occasionally terminals. **b** Section approximately 300 μm more caudal to the section shown in **a**. To the left: a substantial number of terminals in the caudal portion of the anterior hypothalamus, adjacent to the paraventricular hypothalamic nucleus. **c** Enlargement from **b**. Few labeled axons entered the territory of the paraventricular hypothalamic nucleus, with scant terminal labeling. **d** Caudal hypothalamus. To the left: ventral premammillary nucleus; to the right: the caudal portion of the arcuate nucleus, close to the third ventricle. **e** Enlargement from **d**. Abundant terminals filled the neuropil of the ventral premammillary nucleus. **f** Scant terminal labeling in both subdivisions of the arcuate nucleus. The distinct varicosities were connected by very thin intervaricose portions. Scale bar: 50 (**a–c**, **e**, **f**) and 100 μm (**d**).

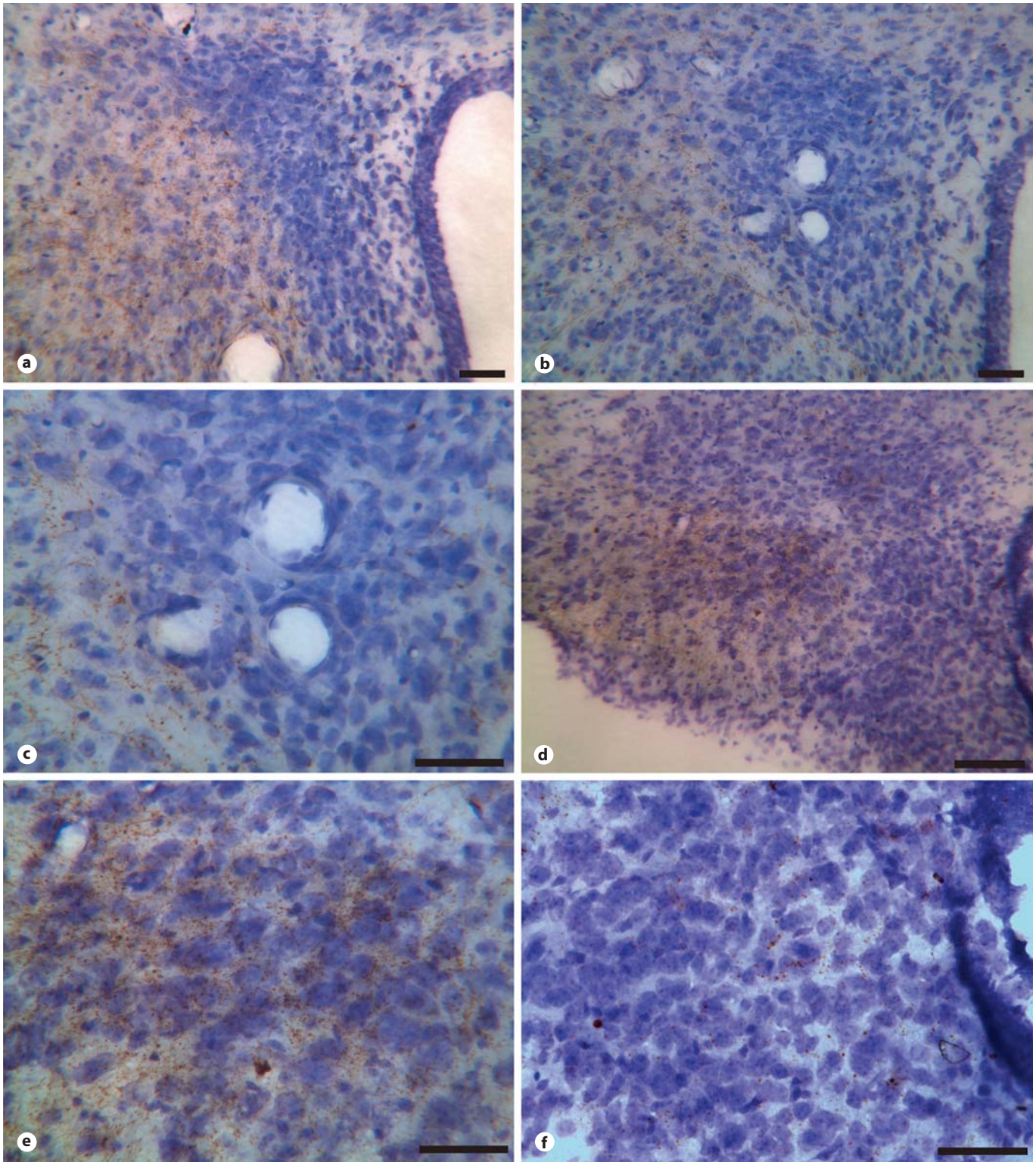

8

distribution of the axonal course and terminal fields. The possibility of a Nissl counterstaining enables both control of the selectivity of the injection and definition of the terminal fields in cytoarchitectonically complicated regions, such as the BST. Due to marginal background staining, very fine details of the axon morphology could be studied. Especially in regions of sparse termination, one is able to follow the collateralization of the labeled axons and to characterize the synaptic terminals. Comparing our results with experiments using Fluoro-Gold, BDA10k is certainly not as effective as the retrograde tracer [Usunoff et al., 2006a, 2007b]. However, neuronal systems with very successful retrograde tracing were noticed in the present study. After discrete injection in the MGP, for example, a very large number of retrogradely labeled medium spiny neurons were observed in the neostriatum. The cells were labeled with a Golgi impregnation-like quality, and even the dendritic spines were visualized.

Injection Foci

Two injections foci were located at the border of the MeA and MePD with diffusion of BDA into the anterior part of the MePD. Therefore, we also analyzed these two animals with MeA-MePD border injections. Interestingly, we observed no obvious differences or trends in the detected efferents of MeA-MePD border injections with regard to the direct MePD injection. Furthermore, the efferents of the MeA-MePD border and the direct MePD injection performed in this study are in accordance with the literature. In the following, the MeA-MePD border and MePD efferents detected in this study are described. However, it should be kept in mind that an overlap of projections that stem from the MeA-MePD border and MePD cannot be excluded.

Efferent Connections of the MePD

The current data indicate that the Me projections in the mouse are comparable to the data obtained in the rat [Canteras et al., 1995], hamster [Kevetter and Winans, 1981; Gomez and Newman, 1992; Coolen and Wood, 1998] and gerbil [Simmons and Yahr, 2002] (table 1). Differences exist with regard to the variable amount of efferent terminals and, in some cases, with the topical distribution of the projections, too.

Intra-Amygdaloid Connections

The injection in the MePD was followed by intensive terminal labeling in the MePV and MeA, and in the latter also retrogradely labeled cells were observed. Very similar findings were seen in the figures of Canteras et al. [1995], and Coolen and Wood [1998]. Within the Am, we followed a moderate number of axons to the BSTIA, intercalated nuclei, and central and basomedial nuclei, but axons entering the anterior Am and the cortical nuclei were only scantily labeled. Our mapping is comparable to the findings of Canteras et al. [1995]. Coolen and Wood [1998] encountered a profuse intra-amygdaloid innervation from the MeP, including the basolateral nucleus; in the latter, our findings were absolutely negative.

Extra-Amygdaloid Connections

The extra-amygdaloid projections of the Me followed two routes: the stria terminalis and the ventral amygdalofugal pathway (ansa peduncularis). In the mouse, the stria terminalis ascended vertically and might be followed on a single coronal section from its origin to the supracapsular part. The labeled Me axons were located in the medial part of the ascending stria. In the supracapsular stria terminalis, the compact bundle of labeled axons was located in its ventromedial part. This position corresponded exactly to the place where NADPH-diaphorase-positive axons of the stria terminalis were situated [Usunoff et al., 2006b: fig. 6b–d]. Also, in the Am, the largest number of NO-producing neurons was to be found in the Me [Pitkänen and Amaral, 1991; McDonald et al., 1993; Paxinos et al., 1999; Usunoff et al., 2006b: fig. 4a, b]. Via the prethalamic descent of the stria terminalis, the labeled stem axons dispersed in numerous axons that formed dense terminal fields in various subdivisions of the BST: BSTMPL (most caudal), BSTMPM, BSTMPI, and most rostral (anterior commissure level), BSTMA and BSTMV. The lateral subdivisions of the BST were ap-

Fig. 9. Projections to the thalamus and epithalamus following injection into the MePD (**a–f**) and the MeA-MePD border (**g**, **h**). **a** To the left: lateral habenular nucleus (LHb); to the right: the medial habenular nucleus (MHb). **b** Enlargement from **a**. Discrete terminals in the lateral habenular nucleus. Occasionally, labeled terminals were close to the border with the medial habenular nucleus (arrows). **c** Moderate terminal labeling in the nucleus reuniens (Re), ipsilateral to the injection. **d** In the same section, occasionally labeled terminals were also present in the contralateral nucleus reuniens [single fibers (arrows) being visible in the magnified region]. **e** Scant terminal clusters in the rhomboid nucleus (Rh). **f** Occasionally, labeled axons in the interanteromedial nucleus (IAM). **g** A small, but condensed terminal field in the lateral portion of the lateral habenular nucleus. **h** Few labeled axons in the zona incerta (ZI). Scale bar: 50 (**a–f**, **h**) and 100 μm (**g**).

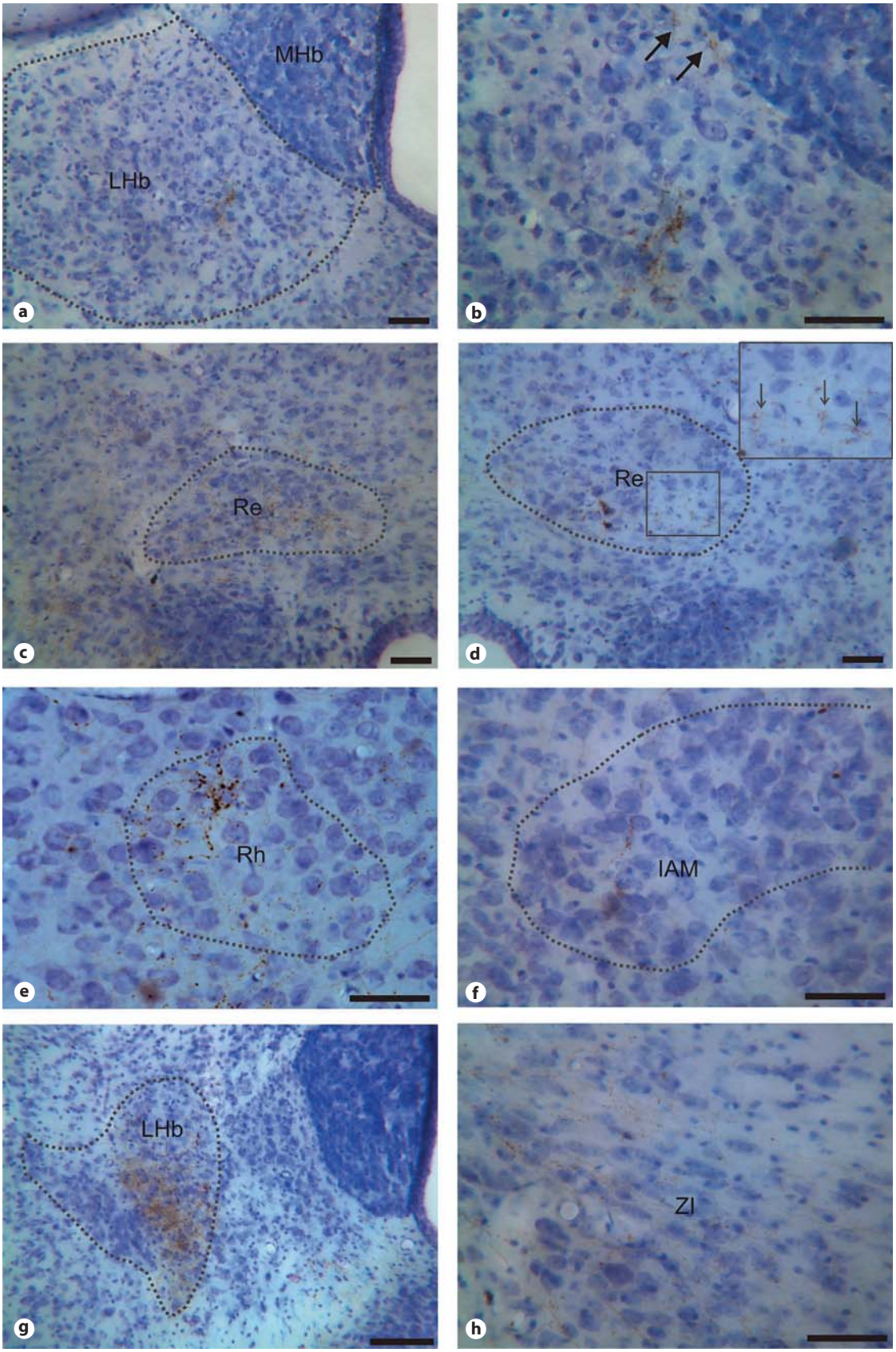

9

parently not innervated by the Me. Recently, we followed BDA-labeled axons to these subdivisions following injection of the tracer in the medial subnucleus of the central amygdaloid nucleus in rats [Usunoff et al., 2007a], and our results were in agreement with the findings of Dong et al. [2001]. A very similar distribution of MePD axons within BST subdivisions was described in the rat [Canteras et al., 1995: fig. 6c–f; Dong et al., 2001: fig. 14a–h], hamster [Coolen and Wood, 1998: fig. 8a–d] and in the gerbil [Simmons and Yahr, 2002: fig. 7a–c] (table 1). The reciprocal connection from the BST to the Me was first suggested by Swanson and Cowan [1976] and recently described in detail by Wood and Swann [2005].

Paxinos and others delineated a neuronal aggregation abutting the ventral aspect of the stria medullaris immediately lateral to the perifornical portion of BSTMPL as a separate structure and named it 'nucleus of stria medullaris' both in the rat [Paxinos and Watson, 1998] and in the mouse [Paxinos and Franklin, 2001]. In all the present experiments, we found a dense field of labeled terminals in the nucleus of the stria medullaris. The stria medullaris also contained a considerable number of straight labeled axons that followed the stream of the bundle, and we traced them to the lateral habenular nucleus. Canteras et al. [1995] and Coolen and Wood [1998] also observed labeled axons in the stria medullaris, but their schematic drawings suggested that only very few and scattered Me axons traveled within this mighty bundle.

We found no labeled axons in the dorsal ('extrapyramidal') striatum, but a fair projection to both core and shell of the nucleus accumbens was evident. Canteras et al. [1995] labeled a sparse projection to the nucleus accumbens from the MeAD, but they followed MeAD and MePD axons to the fundus of the striatum, e.g. to the lateral accumbens shell, as delineated by Paxinos and Franklin [2001]. Coolen and Wood [1998] traced axons to the ventromedial nucleus accumbens after injections in the MeA and MeP. Ventrally to the nucleus accumbens, we followed a moderate amount of labeled axons to the olfactory tubercle. These axons surrounded the islands of Calleja, but only few terminals appeared in their neuropil. Similarly, medial from the nucleus accumbens, labeled axons surrounded the major island ('insula magna' of Calleja). Again, only occasionally terminals were seen within the neurons of this structure. Our observations on the distribution of Me axons in the olfactory tubercle were similar to the schematic drawings of Coolen and Wood [1998].

We traced only a moderate projection from the Me to the septal nuclei. Discrete terminal fields were seen in the ventral portion of the lateral septal nucleus, and in the remaining zones of the lateral septal nucleus only very scant terminals were encountered. We found no projection to the medial septal nucleus. Canteras et al. [1995] were more successful. Also, from the MePD, they traced a substantial number of axons to the lateral septal nucleus, and only a few to the medial septal nucleus. On the other hand, we found a significant number of axons in the septofimbriate nucleus, running parallel to each other towards the triangular septal nucleus, with disproportionately few terminals, surrounding the labeled axons. Such a finding was not reported in previous studies on efferent Me projections.

Grove [1988] investigated afferent SI connections by means of retrograde and anterograde tracing. She stated that the rostral two thirds of the Me sent axons to the ventral SI portions. We traced an appreciable number of axons to the SI also from the MePD, and the projection from the MePD was not negligible, in agreement with the observations of Canteras et al. [1995] and Coolen and Wood [1998]. It remains to be elucidated if the cholinergic neurons of the basal magnocellular nucleus of Meynert [the Ch4 group of Mesulam et al., 1983] are monosynaptically influenced by Me axons. Grove [1988] did not mention such a connection, and the matter was not further discussed in anterograde tracing studies of Me projections. In our preparations, we observed large, hyperchromic neurons in the dorsal SI, adjacent to the internal capsule, that might well be Meynert's neurons, but labeled Me terminals were not traced in close proximity.

The significant connections of the Me with the medial preoptic region have been reported repeatedly [Maragos et al., 1989; Gomez and Newman, 1992; Canteras et al., 1995; Coolen and Wood, 1998; Heeb and Yahr, 2001; Simmons and Yahr, 2002]. Both regions have been implicated in male sexual behavior, and their simultaneous activation during ejaculation has been established [Baum and Everitt, 1992; Coolen et al., 1996, 1998; Parfitt and Newman, 1998; Veening and Coolen, 1998; Newman, 1999; Heeb and Yahr, 2001]. In agreement with the tract-tracing investigations quoted above, in all the present experiments, we followed a large number of axons to the medial preoptic nucleus (lateral and medial subnuclei) and to the medial preoptic area. Notably, in quite a few regions, the number of labeled terminals was larger following MePD than MeA-MePD border injections. The afferent axons arrived as a voluminous, diffuse stream, the medial continuation of the stria terminals axons. We found no firm evidence that axons coursing within the ventral amygdalofugal pathway contributed terminals to the medial preoptic region.

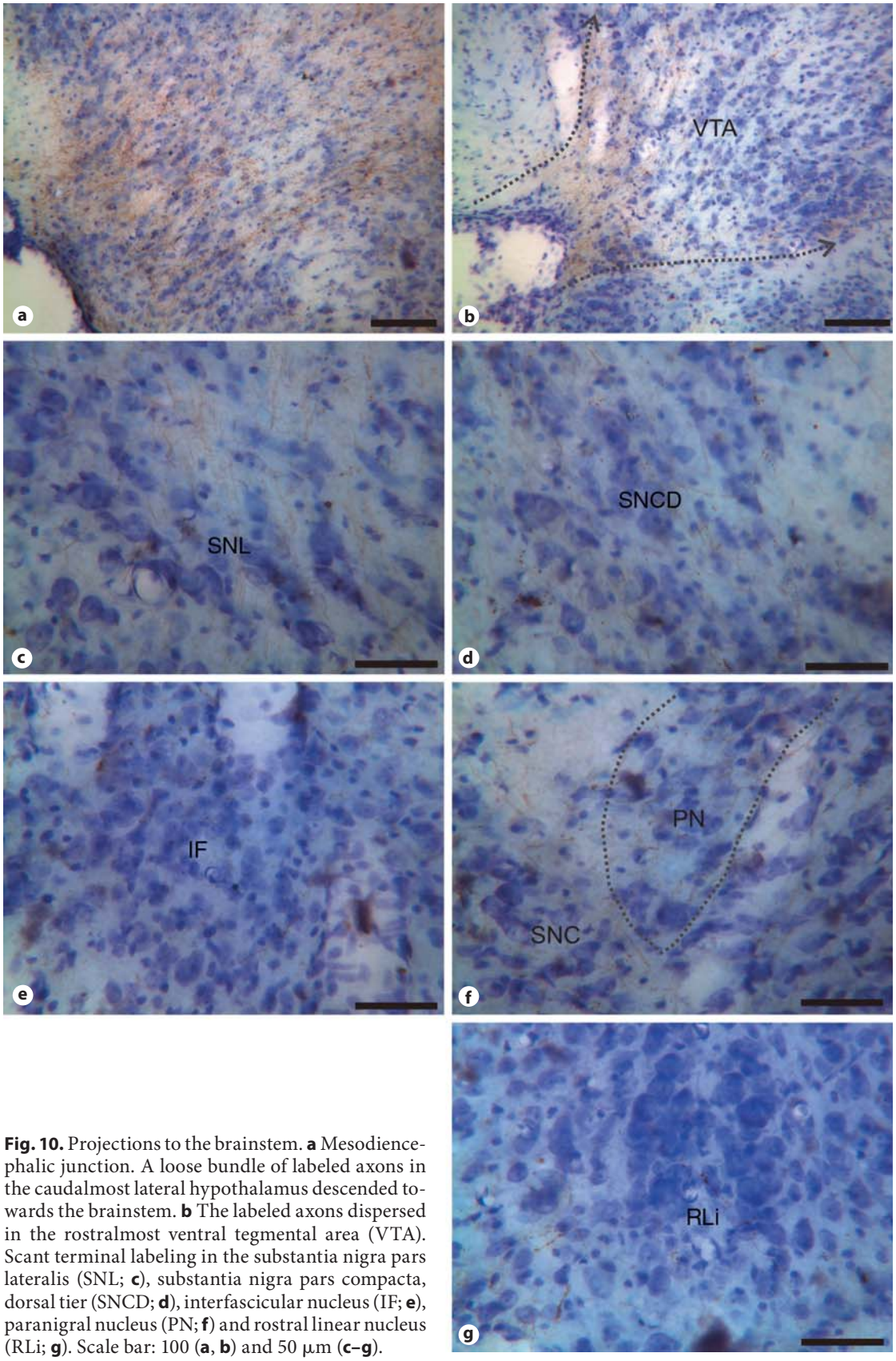

Fig. 10. Projections to the brainstem. **a** Mesodiencephalic junction. A loose bundle of labeled axons in the caudalmost lateral hypothalamus descended towards the brainstem. **b** The labeled axons dispersed in the rostralmost ventral tegmental area (VTA). Scant terminal labeling in the substantia nigra pars lateralis (SNL; **c**), substantia nigra pars compacta, dorsal tier (SNCD; **d**), interfascicular nucleus (IF; **e**), paranigral nucleus (PN; **f**) and rostral linear nucleus (RLi; **g**). Scale bar: 100 (**a**, **b**) and 50 μm (**c**–**g**).

Many structures of the hypothalamus were occupied by labeled axons and terminals but to a variable extent. The anterior hypothalamus contained a moderate number of regularly dispersed axons, but in dorsocaudal direction their number increased significantly and the dense terminal field reached the ventrolateral border of the paraventricular hypothalamic nucleus. According to the present results, both neurosecretory hypothalamic

Table 1. Relative and mean densities (d) of anterograde labeling in the mouse brain produced by BDA injection in the MeA-MePD border (cases 1 and 2) and in the MePD (case 3)

Region	Abbrev.	Case 1	Case 2	Case 3	d	Rat	Hamster	Gerbil
Telencephalon								
Amygdala								
Anterior nucleus	AA	1	1	0	1	1	1	1
Basolateral nucleus	BL	0	0	0	0		0	
Basomedial nucleus	BM	1	1	2	1	1	2	2
Central nucleus	Ce	2	2	3	2	1	3	1
Cortical nuclei	Co	1	1	2	1	3	2	3
Intercalated nuclei	I	2	3	3	3		3	2
Intra-amygdaloid bed nucleus of the stria terminalis	BSTIA	2	1	3	2		3	
Medial nucleus, anterior part	MeA	3	2	1	2		1	3
Medial nucleus, posteroventral part	MePV	3	3	2	3			3
Nucleus of the lateral olfactory tract	LOT	0	1	1	1		0	2
Bed nucleus of the stria terminalis								
Lateral division	BSTL	0	1	0	0		0	
Medial division, anterior part	BSTMA	2	2	2	2	3	2	2
Medial division, posterointermediate part	BSTMPI	2	3	2	2	1	0	3
Medial division, posterolateral part, perifornical sector	BSTMPLps	3	2	1	2	1		
Medial division, posterolateral part, anterior sector	BSTMPLas	0	0	1	0	1		
Medial division, ventral part	BSTMV	2	3	2	2		2	1
Diagonal band nuclei	VDB, HDB	0	0	0	0		0	1
Islands of Calleja	ICj	1	1	2	1			
Nucleus of the stria medullaris	SM	3	2	3	3			
Olfactory tubercle	Tu						0	1
Deep layer	TuOpo	2	2	2	2			
Superficial layers	TuOd, TuOp	1	1	2	1			
Preoptic area								2
Anterodorsal preoptic nucleus	ADP	1	0	2	1			
Lateral preoptic area	LPO	0	1	0	0			
Magnocellular preoptic nucleus	MCPO	0	0	1	0			
Medial preoptic area	MPA	3	2	2	2		2	
Medial preoptic nucleus, lateral part	MPOL	3	2	3	3		3	
Medial preoptic nucleus, medial part	MPOC	3	2	3	3		3	
Septum						1		
Lateral septal nucleus, dorsal part	LSD	0	0	0	0		0	
Lateral septal nucleus, intermediate part	LSI	1	1	1	1		0	
Lateral septal nucleus, ventral part	LSV	2	3	3	3		3	
Septofimbriate nucleus, *axons of passage*	SFi	1	2	2	2			
Triangular septal nucleus	TS	1	0	1	1			
Striatum								
Dorsal striatum	CPu	0	0	1	0		0	
Nucleus accumbens, core	AcbC	1	0	0	0		1	
Nucleus accumbens, shell	AcbSh	2	1	2	2		0	
Substantia innominata						1	0	
Dorsal, axons of passage	SID	1	1	1	1			
Ventral	SIV	3	2	2	2			1

Mean densities are documented in serial sections in figure 13.

Table 1 (continued)

Region	Abbrev.	Case 1	Case 2	Case 3	d	Rat	Hamster	Gerbil
Diencephalon								
Epithalamus								
Lateral habenular nucleus, lateral part	LHbL	2	1	2	2		0	
Lateral habenular nucleus, medial part	LHbM	1	2	3	2		0	
Medial habenular nucleus	MHb	0	0	0	0		0	
Hypothalamus								
Anterior hypothalamic area, anterior part	AHA	1	0	1	1	3	1	1
Anterior hypothalamic area, central part	AHC	3	2	1	2	3	1	
Anterior hypothalamic area, posterior part	AHP	2	2	2	2		2	
Arcuate nucleus	Arc	1	1	1	1	1	1	1
Lateral hypothalamic area	LH	2	3	2	2		0	1
Paraventricular hypothalamic nucleus	Pa	1	2	1	1		1	1
Supraoptic nucleus	So	0	1	2	1			1
Tuber cinereum area	TC	3	2	2	2	1		
Ventral premammillary nucleus	PMV	3	2	1	2	1	1	
Ventromedial hypothalamic nucleus, capsule	VMHCa	3	2	2	2	1	2	
Ventromedial hypothalamic nucleus, central part	VMHC	2	1	1	1	1	0	
Ventromedial hypothalamic nucleus, dorsomedial part	VMHDM	1	0	0	0			
Ventromedial hypothalamic nucleus, ventrolateral part	VMHVL	3	3	3	3	3		2
Thalamus						1	0	
Interanteromedial nucleus	IAM	1	1	0	1			
Nucleus reuniens, ipsilateral	Re	2	1	2	2			
Nucleus reuniens, contralateral	Re	1	0	1	1			
Rhomboid nucleus	Rh	1	2	2	2			
Remaining thalamic nuclei		0	0	0	0			
Mesencephalon								
Dorsal raphe nucleus	DR	1	1	1	1			
Interfascicular nucleus	IF	1	0	1	1			
Periaqueductal gray, lateral part, *axons of passage*	PAG	1	2	3	2	1		
Paranigral nucleus	PN	1	0	1	1			
Rostral linear nucleus of the raphe	RLi	1	1	1	1			
Substantia nigra, pars compacta, dorsal tier	SNCD	1	0	1	1			
Substantia nigra, pars compacta, ventral tier	SNCV	0	0	0	0			
Substantia nigra, pars lateralis	SNL	1	1	1	1			
Substantia nigra, pars reticulata	SNR	0	1	0	0			

The three columns rat [Canteras et al., 1995], hamster [Kevetter and Winans, 1981; Gomez and Newman, 1992; Coolen and Wood, 1998] and gerbil [Simmons and Yahr, 2002] summarize the findings in the publications listed below. Some authors used other nomenclatures or described structures which were not labeled in our work or described only supernuclei like the thalamus or very fine subregions of subnuclei which were not used for comparison in this table. Therefore, not all structures observed by us can be consistently compared. 0 = Absence of labeling; 1 = light labeling; 2 = moderate labeling; 3 = dense labeling.

nuclei received only a very scant innervation from the Me. From all Me injection foci, we followed a dense bundle, coursing immediately dorsal to the supraoptic nucleus, and in this region also a terminal field was regularly observed. However, hardly any Me axon entered the supraoptic nucleus. Only a limited number of labeled axons was charted on the drawings of Canteras et al. [1995], and Coolen and Wood [1998], but in the figures published by Simmons and Yahr [2002], the MePD in gerbils sent an appreciable number of axons within the supraoptic nucleus. We found a slightly more significant number of terminals in the paraventricular hypothalamic nucleus. Tanaka et al. [1997] investigated nitric oxide-producing neurons in the Am projecting to the paraventricular nucleus. They found out that approximately 40% of the neurons projecting to the paraventricular nucleus were nitrergic cells and 16% of NADPH-diaphorase-positive neurons in the Me projected to the paraventricular nu-

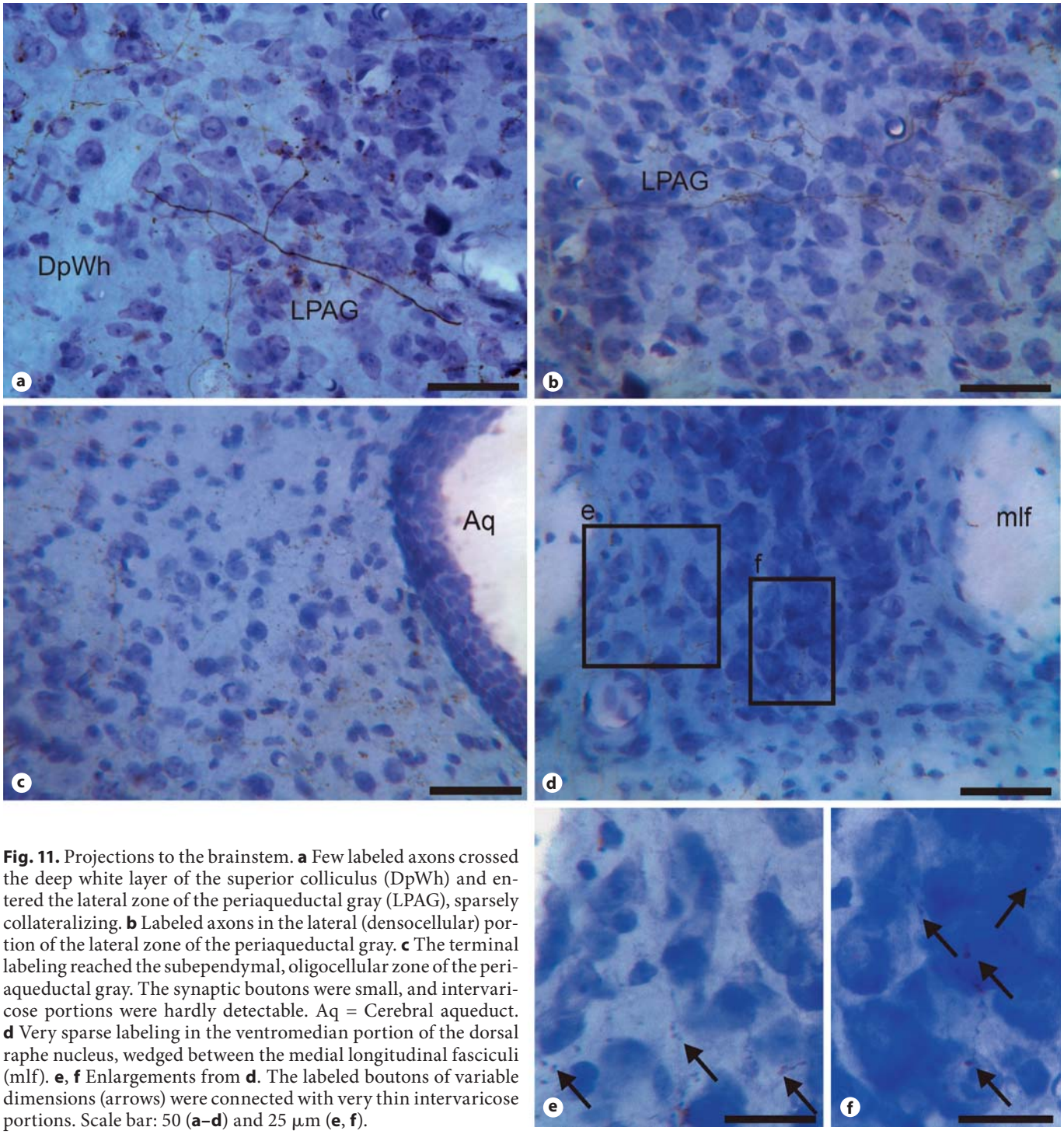

11

Fig. 11. Projections to the brainstem. **a** Few labeled axons crossed the deep white layer of the superior colliculus (DpWh) and entered the lateral zone of the periaqueductal gray (LPAG), sparsely collateralizing. **b** Labeled axons in the lateral (densocellular) portion of the lateral zone of the periaqueductal gray. **c** The terminal labeling reached the subependymal, oligocellular zone of the periaqueductal gray. The synaptic boutons were small, and intervaricose portions were hardly detectable. Aq = Cerebral aqueduct. **d** Very sparse labeling in the ventromedian portion of the dorsal raphe nucleus, wedged between the medial longitudinal fasciculi (mlf). **e**, **f** Enlargements from **d**. The labeled boutons of variable dimensions (arrows) were connected with very thin intervaricose portions. Scale bar: 50 (**a–d**) and 25 μm (**e**, **f**).

Fig. 12. Projections of the MGP. **a** Discrete injection focus in the MGP. The low amount of selectively injected BDA labels the network of the MGP neuropil, interstitial to the unlabeled axons of the internal capsule. Ce = Central amygdaloid nucleus; st = stria terminalis; opt = optic tract; LH = lateral hypothalamic area. **b** Despite the small number of labeled MGP neurons, there was a profuse terminal field in the lateral part of the lateral habenular nucleus (cf. figure 9a, g). **c** Labeled axons in the ventromedial thalamic nucleus. **d** Homogenous but substantial terminal labeling in the parafascicular thalamic nucleus, lateral to the fasciculus retroflexus of Meynert (fr). **e** Few labeled axons in the pars dissipata of the pedunculopontine tegmental nucleus, associated with the axons of the decussating superior cerebellar peduncle. **f** Distinct terminal field in the red nucleus. Scale bar: 200 (**a**), 100 (**b**) and 50 μm (**c–f**).

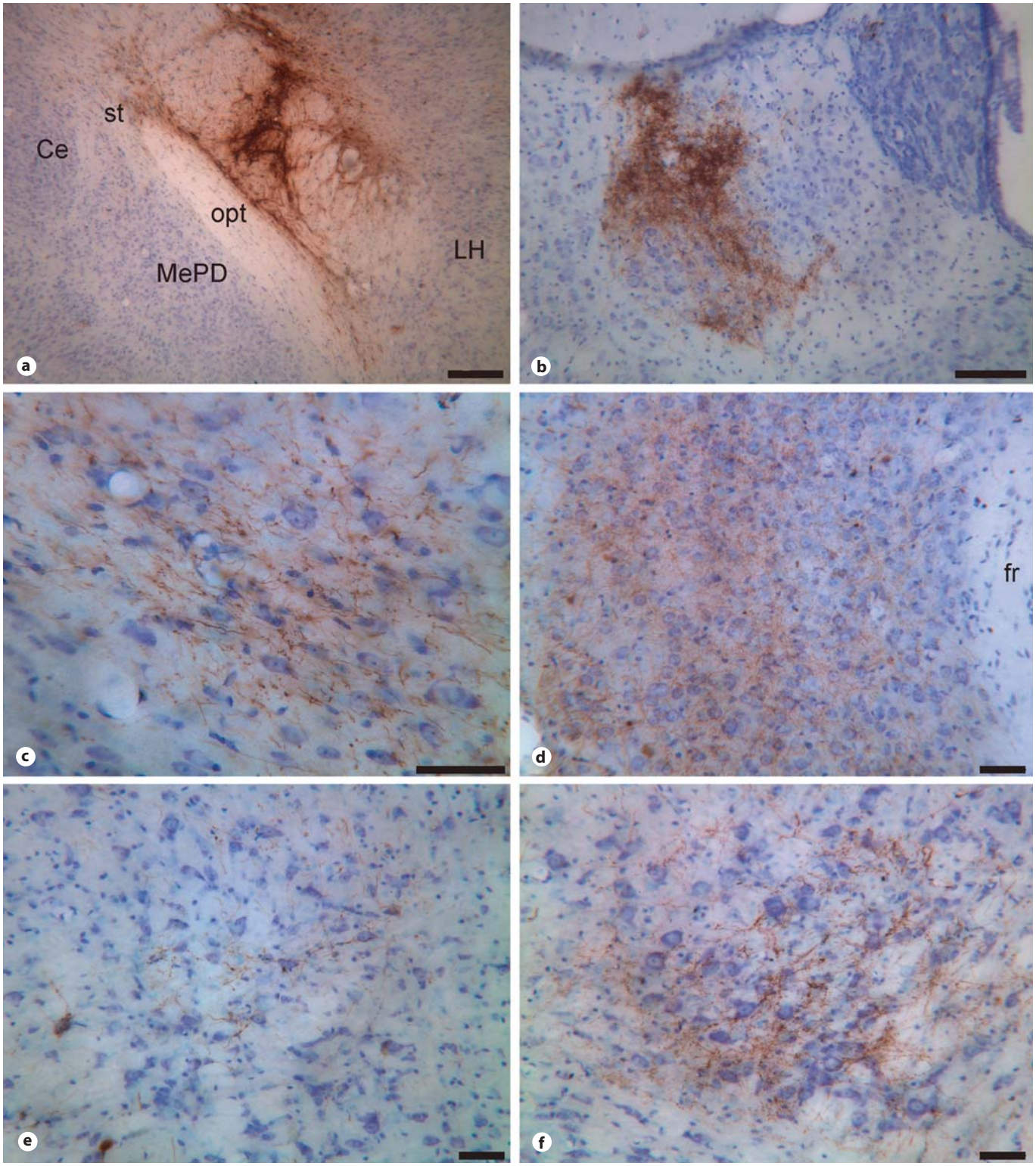

12

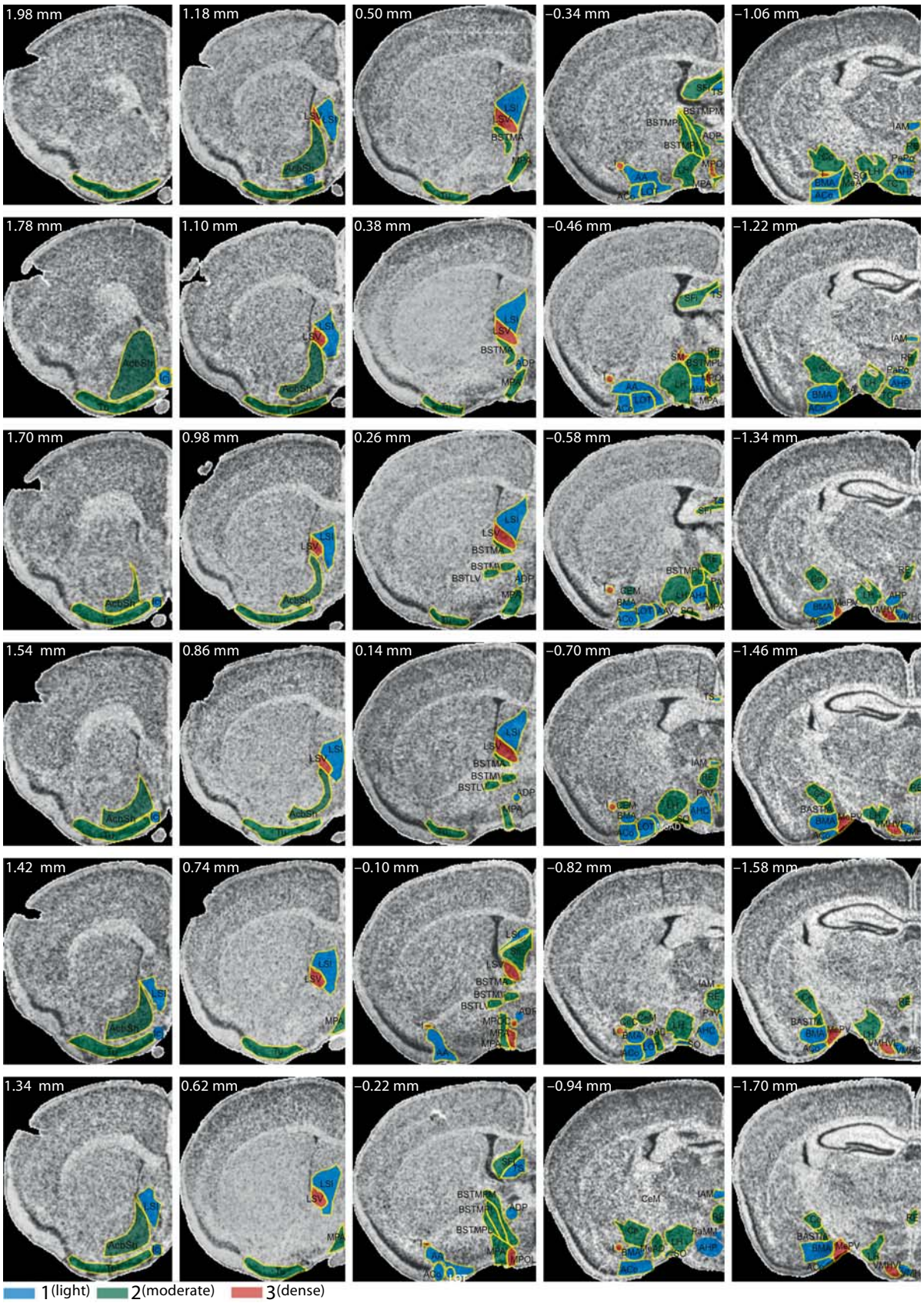
1.98 mm
1.18 mm
0.50 mm
–0.34 mm
–1.06 mm
1.78 mm
1.10 mm
0.38 mm
–0.46 mm
–1.22 mm
1.70 mm
0.98 mm
0.26 mm
–0.58 mm
–1.34 mm
1.54 mm
0.86 mm
0.14 mm
–0.70 mm
–1.46 mm
1.42 mm
0.74 mm
–0.10 mm
–0.82 mm
–1.58 mm
1.34 mm
0.62 mm
–0.22 mm
–0.94 mm
–1.70 mm
1 (light)
2 (moderate)
3 (dense)

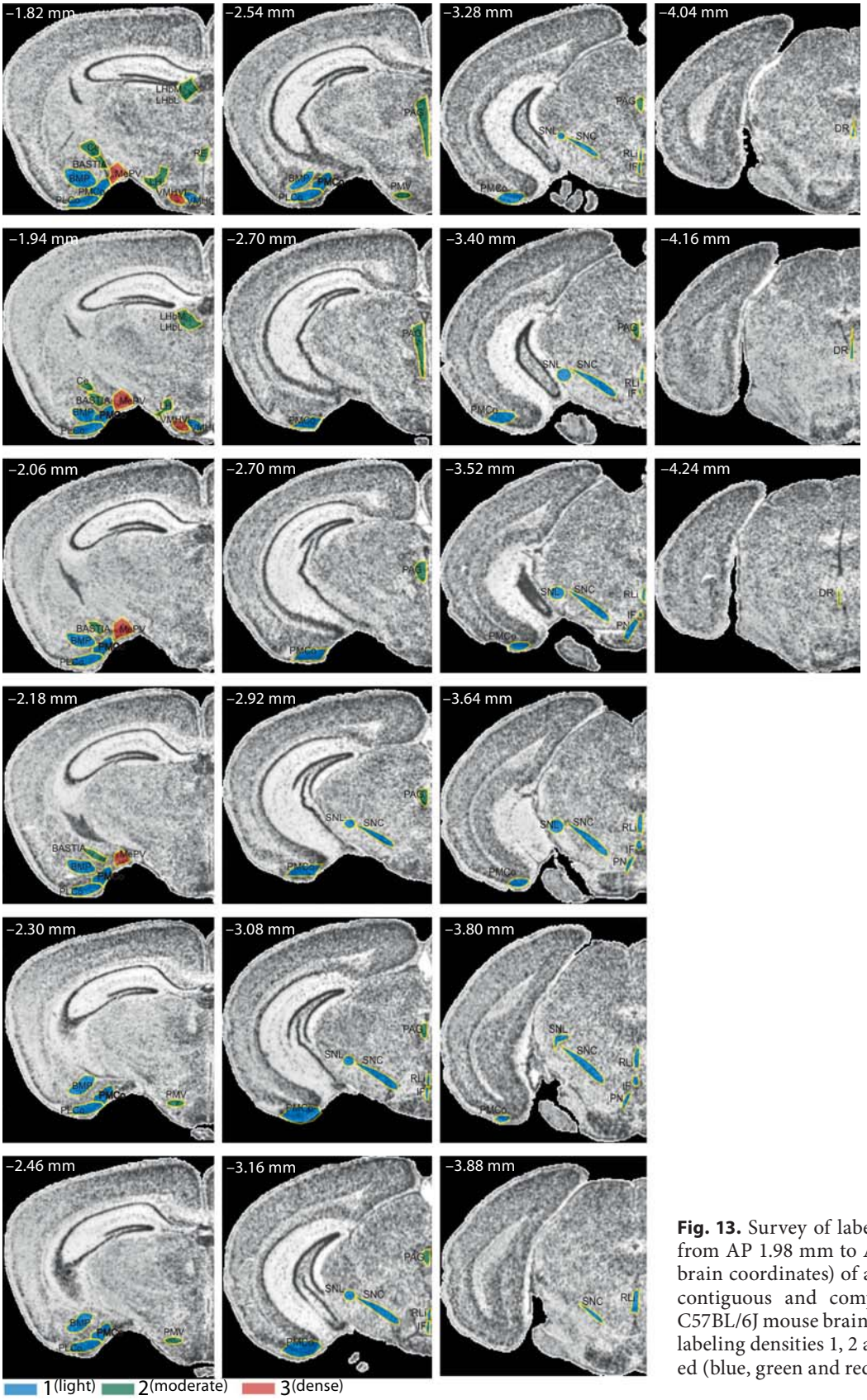

Fig. 13. Survey of labeling densities of all terminals from AP 1.98 mm to AP –4.42 mm (Paxinos mouse brain coordinates) of a mouse brain atlas based on a contiguous and complete histologically sectioned C57BL/6J mouse brain (body weight: 20 g). The mean labeling densities 1, 2 and 3 of table 1 were color coded (blue, green and red, respectively).

cleus. We partially agree with Tanaka et al. [1997]. The nitrergic nature of the Me neurons, as well as their efferent nature, was discussed above. However, the present data do not suggest a significant projection from the Me to the paraventricular hypothalamic nucleus. Moreover, many neurons of this nucleus produced nitric oxide [Yamada et al., 1996; Paxinos et al., 1999: fig. 172 and 179], therefore a further extrinsic nitrergic input would hardly provide an additional influence upon the synaptic events in the paraventricular hypothalamic nucleus.

The data on the VMH innervation by the MeP are somewhat controversial. Gomez and Newman [1992] postulated that the MeA projected to the core of the ventromedial nucleus, and the MeP to its shell (or capsule). According to Canteras et al. [1995], the MeAD heavily innervated the entire VMH, the MePV its central and dorsomedial part, while the MePD supplied, though rather sparsely, only the ventrolateral part. Coolen and Wood [1998] demonstrated a profuse input from the MePD to the ventrolateral part but also a moderate input to the remaining portions of the ventromedial nucleus. Finally, Simmons and Yahr [2002] encountered a sharply delineated terminal field in the ventrolateral part following injections in the MePD. In agreement with all above-quoted investigations, in the present data, the mouse MeA emitted a mighty projection to the entire VMH. Concerning the MePD, our data were largely comparable with the results of Coolen and Wood [1998]. By the MePD injection, the ventral and lateral borders of the VMH were surrounded by a dense terminal field [apparently the shell; Gomez and Newman, 1992], but the latter field was continuous with the field in the ventrolateral part of the VMH. Further, a moderate number of terminals was present in the central part, and even the dorsomedial subnucleus contained few terminals.

In the present study, the descending fibers of the fornix were surrounded by labeled axons and terminals, and on the whole fields were dense in the cases with MeA injections. The findings in the rat were similar [Canteras et al., 1995]. In the Syrian hamster, the labeled Me axons were distributed mainly ventrally and medially to the fornix [Coolen and Wood, 1998], and in the gerbil Simmons and Yahr [2002] traced from the MePD a moderate number of axons, surrounding the lateral aspect of the fornix. In the last decade, the discovery of hypocretin/orexin-containing neurons in the hypothalamus ensued increased attention in the perifornical region [de Lecea et al., 1998; Sakurai et al., 1998]. Surprisingly, this small neuronal population projected to multiple regions throughout the CNS [Peyron et al., 1998; Nambu et al., 1999; van den Pol, 1999; Mintz et al., 2001; Baldo et al., 2003; Stoyanova and Lazarov, 2005], including the Am and BST. Probably, the most important function of hypocretin/orexin is concerned with 'arousal systems' [Jones, 2003; Saper et al., 2005; Ohno and Sakurai, 2008]. The excitatory action of hypocretin/orexin on Am neurons was established by Bisetti et al. [2006]; recently, Muschamp et al. [2007] stressed the involvement of hypocretin/orexin in male sexual behavior.

In agreement with previous reports, we traced a very substantial projection to the ventral premammillary nucleus from the MePD and slightly less from the MeA-MePD border. In our opinion, the comparatively few parent afferent axons from the MePD gave rise to numerous terminal branches, since the density of the terminal field in the ventral premammillary nucleus was comparable to the profuse terminations in the BST, VMH and in the medial preoptic nucleus. The connection from the MePD to the ventral premammillary nucleus represented a significant element of the neuronal network associated with sexual behavior, since its ascending projections reached several structures of the sexually dimorphic circuit [Canteras et al., 1992]. We encountered also a minute projection to both subnuclei of the arcuate nucleus. The few terminals were connected with extremely thin intervaricose portions. This projection was also characterized as modest in previous tracing studies, although the drawings in Coolen and Wood [1998] and in Simmons and Yahr [2002] suggested a rather substantial projection.

Unlike the broad, diverse and often extremely dense innervation of the BST subdivisions, medial preoptic region and of the hypothalamus, the present study evidenced a very scant thalamic innervation, especially by the restricted injection in the MePD. The only more significant target was the lateral habenular nucleus within the epithalamus. Following MeA-MePD border injections, the terminal field was comparable to this after MGP injection. MePD axons were followed mainly to the lateral subnucleus of the lateral habenular nucleus [Paxinos and Franklin, 2001]; in the medial subnucleus, only scant terminals were present, sometimes close to the densely packed neurons of the medial habenular nucleus. Within the latter, no terminals were observed by us though Coolen and Wood [1998] traced few fibers to the medial habenular nucleus, from both the MeA and MeP. Also, Canteras et al. [1995] traced substantial tracts from the MeAD to the nucleus reuniens and to the paraventricular thalamic nucleus, and moderate connections to the zona incerta, parataenial nucleus and mediodorsal nucleus, whilst the data for the MePD were nearly nega-

tive. McKenna and Vertes [2004] examined the afferent connections of the nucleus reuniens and found that a more significant input from Me reached only its rostrolateral part. Also, in this part of the nucleus reuniens, we found only few terminals. We were also not able to trace axons to the mediodorsal thalamic nucleus in the cases with MeA-MePD border injections.

We traced moderate projections to several dopaminergic groups in the hypothalamus and midbrain [Dahlström and Fuxe, 1964; van den Pol et al., 1984]: the posterior part of the anterodorsal preoptic nucleus (group A14), the arcuate nucleus (group A12), the ventral tegmental area (group A10) and the substantia nigra (group A9) presented Me axons, but none of the targets exhibited a substantial number of labeled terminals. Notably, mainly the mesolimbic dopaminergic system was included: the rostral linear, interfascicular and paranigral nucleus [for subdivisions of the ventral tegmental area, see Halliday and Törk, 1986; Paxinos and Franklin, 2001]. In the substantia nigra, only the dorsal tier of the pars compacta (with neurons projecting to the limbic forebrain) and the pars lateralis was sparsely innervated, but not the ventral tier of the pars compacta (containing the nigrostriatal neurons). Except for the arcuate nucleus, in previous investigations, innervation of the dopaminergic nuclei was weak. We found a sparse but morphologically very impressive innervation of the lateral portion of the periaqueductal gray, with individually labeled axons almost reaching the ependyma of the aqueduct. Only occasionally, terminals were noted in the dorsal raphe nucleus. In all probability, the major serotoninergic structure of the CNS had only very limited interconnections with the Me, since Vertes [1991] found no efferent dorsal raphe axons reaching the Me, and we observed only scant retrograde labeling in the dorsal raphe nucleus following voluminous Fluoro-Gold injections in the Me of rats [Usunoff et al., 2006a].

Efferent Connections of the MGP

The discrete injection in the MGP labeled only a limited number of its neurons. However, the MGP efferent projections were successfully traced and, with the exception of a large number of terminals in the lateral habenular nucleus, were entirely different from the pathways traced after the single MePD injection and the two MeA-MePD border injections. All firmly established projections of the MGP were evident: to the thalamic ventromedial and parafascicular nuclei and to the pedunculopontine tegmental nucleus. Parent et al. [2001] pointed out that in primates the lateral habenular nucleus was the most densely innervated pallidal target, in agreement with our data in the mouse brain. An unexpected finding was the terminal field in the ipsilateral red nucleus. The existence of a pallidorubral connection was often promulgated in the classical literature [for comprehensive reviews, see Knook, 1965; Nauta and Mehler, 1966]. Nauta and Mehler [1966] were the first to question the existence of such a connection. In recent reviews [Parent, 1986; Heimer et al., 1995; Parent, 1996; Bolam et al., 2000; Haber and Gdowski, 2004] and in the investigations of efferent projections of the MGP [Hay-Schmidt and Mikkelsen, 1992; Kha et al., 2000; Parent et al., 2001; Parent and Parent, 2004], the red nucleus was not mentioned as a target of pallidal axons. It is implausible that our findings are artificial, e.g. due to anterograde labeling of corticorubral axons. One might exclude this possibility already by the observation of the injection focus, with the labeled MGP neurons and neuropil pierced by the pale, unlabeled axons of the internal capsule. Moreover, although a minimal involvement of corticofugal axons ultimately results in terminal labeling in the pontine nuclei, this was not observed in our experiment. Following the submission of this article, the paper of Pong et al. [2008] appeared. These authors traced BDA-labeled axons from the entopeduncular nucleus to the red nucleus in the cat. Thus, the pallidorubral connection is described in both rodents and carnivores. This connection might be a significant component of a multineuronal chain connecting the basal ganglia with the lower brainstem and spinal cord.

Conclusion

The MePD in the mouse emitted broadly distributed projections to various structures of the forebrain, and only moderate projections to the rostral brainstem. The most significant tracts were destined to the BST, in which practically all parts of the medial division were innervated by MePD neurons. Moderate projections were evident to the limbic striatum (nucleus accumbens), olfactory tubercle and the lateral septal nucleus. The SI was also innervated by the MePD, and the projection to its ventral portion was substantial. The profuse innervation of the medial preoptic nucleus and medial preoptic area indicated significant involvement of the MePD in sexual behavior. The dependence of the MePD volume and cell size on circulating gonadal hormones in rats [Cooke et al., 1999; Hermela et al., 2006] and mice [Morrisa et al., 2008] was emphasized, however, changes in the axon density were not reported in these studies. Furthermore, many hypothalamic nuclei were innervated but to a different

extent. The very strong innervation of the ventral premammillary nucleus further indicated the involvement of the MePD in the neuronal circuitry for sexual behavior. Substantial projections also reached the anterior hypothalamus and tuber cinereum, while the connection to the lateral hypothalamus was widespread but with moderate density. MePD strongly innervated the ventrolateral VMH subnucleus, but in other subnuclei terminals were also present. Only a small number of axons entered the arcuate nucleus and the neurosecretory hypothalamic nuclei. The thalamic innervation was sparse and reached the epithalamic lateral habenular nucleus and the nuclei of the midline. The mesencephalic connections were scant and reached the limbic dopaminergic groups, the periaqueductal gray and the dorsal raphe nucleus. The present results were comparable to available data on other rodent species, although MePD efferents often differed in extent and/or topical distribution.

Acknowledgments

The expert technical assistance of Mrs. Barbara Kuhnke (Rostock), Ekaterina A. Zlatanova, Snejina S. Ilieva and Elena I. Ivanova (Sofia) is gratefully acknowledged. This work was partially supported by the National Science Fund of the Ministry of Education and Science of Bulgaria (project No. DOL-786/2007).

References

Aggleton, J.P. (1992) The Amygdala: Neurobiological Aspects of Emotion, Memory and Mental Dysfunction. New York, Wiley-Liss.

Aggleton, J.P. (2000) The Amygdala: A Functional Analysis, ed 2. Oxford, Oxford University Press.

Aizawa, H., Y. Sato, M. Maekawa, H. Fujisawa, T. Hirata, S. Yuasa (2004) Development of the amygdalohypothalamic projection in the mouse embryonic forebrain. Anat Embryol (Berl) *208:* 249–264.

Amaral, D.G., J.L. Price, A. Pitkänen, S.T. Carmichael (1992) Anatomical organization of the primate amygdaloid complex; in Aggleton, J.P. (ed): The Amygdala: Neurobiological Aspects of Emotion, Memory and Mental Dysfunction. New York, Wiley-Liss, pp 1–66.

Baldo, B.A., R.A. Daniel, C.W. Berridge, A.E. Kelley (2003) Overlapping distributions of orexin/hypocretin- and dopamine-β-hydroxylase immunoreactive fibers in rat brain regions mediating arousal, motivation, and stress. J Comp Neurol *464:* 220–237.

Barber, P.C. (1982) Adjacent laminar terminations of two centrifugal afferent pathways to the accessory olfactory bulb in the mouse. Brain Res *245:* 215–221.

Barber, P.C., P.M. Field (1975) Autoradiographic demonstration of afferent connections of the accessory olfactory bulb in the mouse. Brain Res *85:* 201–203.

Baum, M.J., B.J. Everitt (1992) Increased expression of c-fos in the medial preoptic area after mating in male rats: role of afferent inputs from the medial amygdala and midbrain central tegmental field. Neuroscience *50:* 627–646.

Ben-Ari, Y. (1981) The Amygdaloid Complex. Amsterdam, Elsevier.

Bisetti, A., V. Cvetkovic, M. Serafin, L. Bayer, D. Machard, B.E. Jones, M. Mühlethaler (2006) Excitatory action of hypocretin/orexin on neurons of the central medial amygdala. Neuroscience *142:* 999–1004.

Bolam, J.P., J.J. Hanley, P.A. Booth, M.D. Bevan (2000) Synaptic organization of the basal ganglia. J Anat *196:* 527–542.

Canteras, N.S., R.B. Simerly, L.W. Swanson (1992) Projections of the ventral premammillary nucleus. J Comp Neurol *324:* 195–212.

Canteras, N.S., R.B. Simerly, L.W. Swanson (1995) Organization of projections from the medial nucleus of the amygdala: a PHAL study in the rat. J Comp Neurol *360:* 213–245.

Cooke, B.M., G. Tabibnia, S.M. Breedlove (1999) A brain sexual dimorphism controlled by adult circulating androgens. Proc Natl Acad Sci USA *96:* 7538–7540.

Coolen, L.M., H.T. Jansen, R.L. Goodman, R.I. Wood, M.N. Lehman (1999) A new method for simultaneous demonstration of anterograde and retrograde connections in the brain: co-injections of biotinylated dextran amine and the beta subunit of cholera toxin. J Neurosci Methods *91:* 1–8.

Coolen, L.M., H.J.P.W. Peters, J.G. Veening (1996) Fos immunoreactivity in the rat brain following consummatory elements of sexual behavior: a sex comparison. Brain Res *738:* 67–82.

Coolen, L.M., H.J.P.W. Peters, J.G. Veening (1998) Anatomical interrelationships of the medial preoptic area and other brain regions activated following male sexual behavior: a combined fos and tract-tracing study. J Comp Neurol *397:* 421–435.

Coolen, L.M., R.L. Wood (1998) Bidirectional connections of the medial amygdaloid nucleus in the Syrian hamster brain: simultaneous anterograde and retrograde tract tracing. J Comp Neurol *399:* 189–209.

Dahlström, A., K. Fuxe (1964) Evidence for the existence of monoamine-containing neurons in the central nervous system. I. Demonstration of monoamines in the cell bodies of brainstem neurons. Acta Physiol Scand *62(suppl 232):* 1–55.

de Lecea, L., T.S. Kilduff, C. Peyron, X. Gao, P.E. Foye, P.E. Danielson, C. Fukuhara, E.L. Battenberg, V.T. Gautvik, F.S. Bartlett, W.N. Frankel, A.N. van den Pol, F.E. Bloom, K.M. Gautvik, J.G. Sutcliffe (1998) The hypocretins: hypothalamus-specific peptides with neuroexcitatory activity. Proc Natl Acad Sci USA *95:* 322–327.

de Olmos, J.S. (1990) Amygdala; in Paxinos, G. (ed): The Human Nervous System. San Diego, Academic Press, pp 583–710.

de Olmos, J.S. (2004) Amygdala; in Paxinos, G., J.K. Mai (eds): The Human Nervous System, ed 2. San Diego, Elsevier/Academic Press, pp 739–868.

de Olmos, J.S., G.F. Alheid, C.A. Beltramino (1985) Amygdala; in Paxinos, G. (ed): The Rat Nervous System, vol 1: Forebrain and Midbrain. New York, Academic Press, pp 223–234.

de Olmos, J.S., C.A. Beltramino, G.F. Alheid (2004) Amygdala and extended amygdala: a cytoarchitectonical, fibroarchitectonical, and chemoarchitectonical survey; in Paxinos, G. (ed): The Rat Nervous System, ed 3. San Diego, Elsevier/Academic Press, pp 509–609.

Dong, H.-W., G.D. Petrovich, L.W. Swanson (2001) Topography of projections from amygdala to bed nuclei of the stria terminalis. Brain Res Rev *38:* 192–246.

Eleftheriou, B. (1973) The Neurobiology of the Amygdala. New York, Plenum Press.

Gomez, D.M., S.W. Newman (1992) Differential projections of the anterior and posterior regions of the medial amygdaloid nucleus in the Syrian hamster. J Comp Neurol *317:* 195–218.

Grove, E.A. (1988) Neural associations of the substantia innominata in the rat. J Comp Neurol *277:* 315–346.

Haber, S.N., M.J. Gdowski (2004) The basal ganglia; in Paxinos, G., J.K. Mai (eds): The Human Nervous System, ed 3. San Diego, Elsevier/Academic Press, pp 676–738.

Halliday, G.M., I. Törk (1986) Comparative anatomy of the ventromedial mesencephalic tegmentum in the rat, cat, monkey and human. J Comp Neurol *252:* 423–445.

Hay-Schmidt, A., J.D. Mikkelsen (1992) Demonstration of a neuronal projection from the entopeduncular nucleus to the substantia nigra of the rat. Brain Res *576:* 343–347.

Heeb, M.M., P. Yahr (2001) Anatomical and functional connections among cell groups in the gerbil brain that are activated with ejaculation. J Comp Neurol *439:* 248–258.

Heimer, L., D.S. Zahm, G.R. Alheid (1995) Basal ganglia; in Paxinos, G. (ed): The Rat Nervous System, ed 2. San Diego, Academic Press, pp 579–628.

Hermela, E.E.S., J. Ilhaa, L.L. Xavierc, A.A. Rasia-Filhoa, M. Achavala (2006) Influence of sex and estrous cycle, but not laterality, on the neuronal somatic volume of the posterodorsal medial amygdala of rats. Neurosci Lett *405:* 153–158.

Holstege, G., J.R. Georgiadis, A.M. Paans, L.C. Meiners, F.H. van der Graaf, A.A. Reinders (2003) Brain activation during human male ejaculation. J Neurosci *23:* 9185–9193.

Jones, B.E. (2003) Arousal systems. Front Biosci *8:* 438–451.

Kevetter, G.A., S.S. Winans (1981) Connections of the corticomedial amygdala in the golden hamster. I. Efferents of the 'vomeronasal amygdala'. J Comp Neurol *197:* 81–98.

Kha, H.T., D.I. Finkelstein, D.V. Pow, A.J. Lawrence, M.K. Horne (2000) Study of projections from the entopeduncular nucleus to the thalamus of the rat. J Comp Neurol *426:* 366–377.

Knook, H.L. (1965) The Fibre Connections of the Forebrain; thesis. Leiden, Van Gorcum.

Lanciego, J.L., F.G. Wouterlood, E. Erro, J. Arribas, N. Gonzalo, X. Urra, S. Cervantes, J.M. Gimenez-Amaya (2000) Complex brain circuits studied via simultaneous and permanent detection of three transported neuroanatomical tracers in the same histological section. J Neurosci Methods *103:* 127–135.

Maragos, W.F., S.W. Newman, M.N. Lehman, J.B. Powers (1989) Neurons of origin and fiber trajectory of amygdalofugal projections to the medial preoptic area in Syrian hamsters. J Comp Neurol *280:* 59–71.

McDonald, A.J. (1992) Cell types and intrinsic connections of the amygdala; in Aggleton, J.P. (ed): The Amygdala: Neurobiological Aspects of Emotion, Memory, and Mental Dysfunction. New York, Wiley-Liss, pp 67–96.

McDonald, A.J. (2003) Is there an amygdala, and how far does it extend? An anatomical perspective. Ann NY Acad Sci *985:* 1–21.

McDonald, A.J., D.R. Payne, F. Mascagni (1993) Identification of putative nitric oxide producing neurons in the rat amygdala using NADPH-diaphorase histochemistry. Neuroscience *52:* 97–106.

McKenna, J.T., R.T. Vertes (2004) Afferent projections to nucleus reuniens of the thalamus. J Comp Neurol *480:* 115–142.

Mesulam, M.-M., E.J. Mufson, B.H. Wainer, A.I. Levey (1983) Central cholinergic pathways in the rat: an overview based on an alternative nomenclature (Ch1-Ch6). Neuroscience *10:* 1185–1201.

Mintz, E.M., A.N. van den Pol, A.A. Casano, H.E. Albers (2001) Distribution of hypocretin-(orexin) immunoreactivity in the central nervous system of Syrian hamsters *(Mesocricetus auratus).* J Chem Neuroanat *21:* 225–238.

Miyashita, T., N. Ichinohe, K.S. Rockland (2007) Differential modes of termination of amygdalothalamic and amygdalocortical projections in the monkey. J Comp Neurol *502:* 309–324.

Morris, J.A., C.L. Jordan, Z.A. King, K.V. Northcutt, S.M. Breedlove (2008) Sexual dimorphism and steroid responsiveness of the posterodorsal medial amygdala in adult mice. Brain Res *1190:* 115–121.

Muschamp, J.W., J.M. Dominguez, S.M. Sato, R.-Y. Shen, E.M. Hull (2007) A role for hypocretin (orexin) in male sexual behavior. J Neurosci *27:* 2837–2845.

Nambu, T., T. Sakurai, K. Mizukami, Y. Hosoya, M. Yanagisawa, K. Goto (1999) Distribution of orexin neurons in the adult rat brain. Brain Res *827:* 243–260.

Nauta, W.J.H., W.R. Mehler (1966) Projections of the lentiform nucleus in the monkey. Brain Res *1:* 3–42.

Newman, S.W. (1999) The medial extended amygdala in male reproductive behavior – a node in the mammalian social behavior network. Ann NY Acad Sci *877:* 242–257.

Oades, R.D., G.M. Halliday (1987) Ventral tegmental (A10) system: neurobiology. 1. Anatomy and connectivity. Brain Res *434:* 117–165.

Ohno, K., T. Sakurai (2008) Orexin neuronal circuitry: role in the regulation of sleep and wakefulness. Front Neuroendocrinol *29:* 70–87.

Parent, A. (1986) Comparative Neurobiology of the Basal Ganglia. New York, Wiley.

Parent, A. (1996) Carpenter's Human Neuroanatomy, ed 9. Baltimore, Williams & Wilkins.

Parent, M., M. Lévesque, A. Parent (2001) Two types of projection neurons in the internal pallidum of primates: single-axon tracing and three-dimensional reconstruction. J Comp Neurol *439:* 162–175.

Parent, M., A. Parent (2004) The pallidofugal motor fiber system in primates. Parkinsonism Relat Disord *10:* 203–211.

Parfitt, D.B., S.W. Newman (1998) Fos-immunoreactivity within the extended amygdala is correlated with the onset of sexual satiety. Horm Behav *34:* 17–29.

Paxinos, G., K.B.J. Franklin (2001) The Mouse Brain in Stereotaxic Coordinates, ed 2. San Diego, Academic Press.

Paxinos, G., L. Kus, K.W.S. Aschwell, C. Watson (1999) Chemoarchitectonic Atlas of the Rat Forebrain. San Diego, Academic Press.

Paxinos, G., C. Watson (1998) The Rat Brain in Stereotaxic Coordinates, ed 4. San Diego, Academic Press.

Peyron, C., D.K. Tighe, A.N. van den Pol, L. de Lecea, H.C. Heller, J.G. Sutcliffe, T.S. Kilduff (1998) Neurons containing hypocretin (orexin) project to multiple neuronal systems. J Neurosci *18:* 9996–10015.

Pickel, V.M., E.J. Van Bockstaele, J. Chan, D.M. Cestari (1996) GABAergic neurons in rat nuclei of solitary tracts receive inhibitory-type synapses from amygdaloid efferents lacking detectable GABA-immunoreactivity. J Neurosci Res *44:* 446–458.

Pitkänen, A. (2000) Connectivity of the rat amygdaloid complex; in Aggleton, J.P. (ed): The Amygdala. A Functional Analysis, ed 2. Oxford, Oxford University Press, pp 31–115.

Pitkänen, A., D.G. Amaral (1991) Distribution of reduced nicotinamide adenine dinucleotide diaphorase (NADPH-d) cells and fibers in the monkey amygdaloid complex. J Comp Neurol *313:* 326–348.

Pong, M., K.M. Horn, A.R. Gibson (2008) Pathways for control of face and neck musculature by the basal ganglia and cerebellum. Brain Res Rev *58:* 249–264.

Price, J.L., F.T. Russchen, D.G. Amaral (1987) The limbic region: II: the amygdaloid complex; in Björklund, A., T. Hökfelt, L.W. Swanson (eds): Handbook of Chemical Neuroanatomy, vol 5: Integrated Systems of the CNS. Part I. Amsterdam, Elsevier, pp 289–381.

Reiner, A., C.L. Veenman, L. Medina, Y. Jiao, N. Del Mar, M.G. Honig (2000) Pathway tracing using biotinylated dextran amines. J Neurosci Methods *103:* 23–37.

Sakurai, T., A. Amemiya, M. Ishii, I. Matsuzaki, R.M. Chemelli, H. Tanaka, S.C. Williams, J. A. Richardson, G.P. Kozlowski, S. Wilson, J.R. Arch, R.E. Buckingham, A.C. Haynes, S.A. Carr, R.S. Annan, D.E. McNulty, W.S. Liu, J.A. Terrett, N.E. Elshourbagy, D.J. Bergsma, M. Yanagisawa (1998) Orexins and orexin receptors: a family of hypothalamic neuropeptides and G protein-coupled receptors that regulate feeding behavior. Cell *92:* 573–585.

Salazar, I., P.A. Brennan (2001) Retrograde labeling of mitral/tufted cells in the mouse accessory olfactory bulb following local injections of the lipophilic tracer DiI into the vomeronasal amygdala. Brain Res *896:* 198–203.

Saper, C.B., Scammell T.E., J. Lu (2005) Hypothalamic regulation of sleep and circadian rhythms. Nature *437:* 1257–1263.

Shipley, M.T., G.D. Adamek (1984) The connections of the mouse olfactory bulb: a study using orthograde and retrograde transport of wheat germ agglutinin conjugated to horseradish peroxidase. Brain Res Bull *12:* 669–688.

Shipley, M.T., Y. Geinisman (1984) Anatomical evidence for convergence of olfactory, gustatory, and visceral afferent pathways in mouse cerebral cortex. Brain Res Bull *12:* 221–226.

Smith, B.S., O.E. Millhouse (1985) The connections between the basolateral and central amygdaloid nuclei. Neurosci Lett *56:* 307–309.

Simmons, D.A., P. Yahr (2002) Projections of the posterodorsal preoptic nucleus and the lateral part of the posterodorsal medial amygdala in male gerbils, with emphasis on cells activated with ejaculation. J Comp Neurol *444:* 75–94.

Simmons, D.A., P. Yahr (2003) GABA and glutamate in mating-activated cells in the preoptic area and medial amygdala of male gerbils. J Comp Neurol *459:* 290–300.

Stoyanova, I.I., N.E. Lazarov (2005) Localization of orexin-A-immunoreactive fibers in the mesencephalic trigeminal nucleus of the rat. Brain Res *1054:* 82–87.

Swanson, L.W. (2003) The amygdala and its place in the cerebral hemisphere. Ann NY Acad Sci *985:* 174–184.

Swanson, L.W., W.M. Cowan (1976) The connections of the septal region. J Comp Neurol *185:* 621–656.

Tanaka, M., T. Ikeda, S. Havashi, N. Iijima, F. Amaya, Y. Hisa, Y. Ibata (1997) Nitrergic neurons in the medial amygdala project to the hypothalamic paraventricular nucleus of the rat. Brain Res *777:* 13–21.

Usunoff, K.G., D.E. Itzev, N.E. Lazarov, O. Schmitt, A. Rolfs, A. Wree (2007a) Interconnections between the central amygdaloid nucleus and the bed nucleus of stria terminalis in the rat. Anterograde and retrograde tracing study. CR Acad Bulg Sci *60:* 1127–1132.

Usunoff, K.G., D.E. Itzev, A. Rolfs, O. Schmitt, A. Wree (2006a) Brain stem afferent connections of the amygdala in the rat with special references to a projection from the parabigeminal nucleus: a fluorescent retrograde tracing study. Anat Embryol *211:* 475–496.

Usunoff, K.G., D.E. Itzev, A. Rolfs, O. Schmitt, A. Wree (2006b) Nitric oxide synthase-containing neurons in the amygdaloid nuclear complex of the rat. Anat Embryol *211:* 721–737.

Usunoff, K.G., O. Schmitt, D.E. Itzev, A. Rolfs, A. Wree (2007b) Efferent connections of the parabigeminal nucleus to the amygdala and the superior colliculus in the rat: a double-labeling fluorescent retrograde tracing study. Brain Res *1133:* 87–91.

van den Pol, A.N., (1999) Hypothalamic hypocretin (orexin): robust innervation of the spinal cord. J Neurosci *19:* 3171–3182.

van den Pol, A.N, R.S. Herbst, J.F. Powell (1984) Tyrosine hydroxylase-immunoreactive neurons of the hypothalamus: a light and electron microscopic study. Neuroscience *13:* 1117–1156.

Veening, J.G., L.M. Coolen (1998) Neural activation following sexual behavior in the male and female rat brain. Behav Brain Res *92:* 181–193.

Vertes, R.P. (1991) A PHA-L analysis of ascending projections of the dorsal raphe nucleus in the rat. J Comp Neurol *313:* 643–668.

Wood, R.I., S.W. Newman (1995) Hormonal influence on neurons of the mating behavior pathway in male hamsters; in Micevych, P., R.P. Hammer (eds): Neurobiological Effects of Sex Steroid Hormones. Cambridge, Cambridge University Press, pp 3–39.

Wood, R.I., J.M. Swann (2005) The bed nucleus of the stria terminalis in the Syrian hamster: subnuclei and connections of the posterior division. Neuroscience *135:* 155–179.

Yamada, K., P. Emson, T. Hökfelt (1996) Immunohistochemical mapping of nitric oxide synthase in the rat hypothalamus and colocalization with neuropeptides. J Chem Neuroanat *10:* 295–316.